nature geoscience

REVIEW ARTICLE

PUBLISHED ONLINE: 27 NOVEMBER 2011 | DOI: 10.1038/NGEO1328

Role of the deep mantle in generating the compositional asymmetry of the Hawaiian mantle plume

Dominique Weis[1,2], Michael O. Garcia[3], J. Michael Rhodes[4], Mark Jellinek[1] and James S. Scoates[1,2]

Linear chains of volcanic ocean islands are one of the most distinctive features on our planet. The longest, the Hawaiian–Emperor Chain, has been active for more than 80 million years, and is thought to have formed as the Pacific Plate moved across the Hawaiian mantle plume, the hottest and most productive of Earth's plumes. Volcanoes fed by the plume today form two adjacent trends, including Mauna Kea and Mauna Loa, that exhibit strikingly different geochemical characteristics. An extensive data set of isotopic analyses shows that lavas with these distinct characteristics have erupted in parallel along the Kea and Loa trends for at least 5 million years. Seismological data suggest that the Hawaiian mantle plume, when projected into the deep mantle, overlies the boundary between typical Pacific lower mantle and a sharply defined layer of apparently different material. This layer exhibits low seismic shear velocities and occurs on the Loa side of the plume. We conclude that the geochemical differences between the Kea and Loa trends reflect preferential sampling of these two distinct sources of deep mantle material. Similar indications of preferential sampling at the limit of a large anomalous low-velocity zone are found in Kerguelen and Tristan da Cunha basalts in the Indian and Atlantic oceans, respectively. We infer that the anomalous low-velocity zones at the core–mantle boundary are storing geochemical anomalies that are enriched in recycled material and sampled by strong mantle plumes.

Mantle plumes and their related hotspot volcanism constitute one of the main processes affecting the cooling and internal differentiation of the Earth's mantle and crust. The mantle plumes form in response to cooling of the Earth's core[1,2]. Whereas plume heads contribute huge volumes of lava to the Earth's surface over short periods of time, plume tails create chains of volcanoes, some extending for thousands of kilometres. For example, Hawai'i in the Pacific Ocean (Fig. 1a) and Kerguelen and Réunion in the Indian Ocean are three mantle plumes associated with long surface tracks that represent important features of the Earth's lithosphere[3]. Mantle plumes may originate in the lower mantle[4], from near the core–mantle boundary (CMB)[5–7], and decompression of the rising material generates melting at shallow depth as it approaches the surface[5].

Geochemical studies of ocean island basalts (OIB) brought to the surface by a deep mantle plume indicate that the Earth's mantle is chemically and isotopically heterogeneous at scales ranging from centimetres to thousands of kilometres[8–11] and provide essential information about its composition and evolution. OIBs present different isotopic compositions. Radiogenic isotopic ratios (a 'fingerprint' of their mantle source) show that these differences result from time-integrated evolution, over millions to billions of years, of compositionally distinct source regions with different history and parent–daughter fractionation[11,12]. Radioactive isotope parents (^{87}Rb, ^{147}Sm, ^{176}Lu, ^{238}U, ^{235}U and ^{232}Th) decay with a very long half-life into daughter isotopes (in our case ^{87}Sr, ^{143}Nd, ^{176}Hf, ^{206}Pb, ^{207}Pb and ^{208}Pb, respectively). As a result the daughter isotope ratios reflect the long-term history of the basalt-source reservoirs in the mantle: they are the 'fingerprint' of their mantle sources. Systematic relationships of OIB compositions in binary isotopic diagrams are commonly interpreted as resulting from mixing between well-defined mantle endmembers[9,13]. These endmembers, expressed at the surface in OIB, do not correspond to any systematic geographical distribution (Fig. 1b). For example, EM-I (enriched mantle type-I) signatures are found in basalts from Indian, south Atlantic and Pacific islands, and HIMU (high U/Pb) signatures in basalts from Atlantic and Pacific islands.

These 'mantle reservoirs' probably reflect contributions from both the early solidification and differentiation of the Earth's mantle[14,15] as well as minor contributions from sediments, oceanic crust and continental crust, and sublithospheric mantle introduced into the deep mantle by subduction and plate-scale mantle stirring[16,17]. The presence of specific and traceable components in the mantle source of oceanic basalts provides a framework for discussing the origins of mantle plumes, the source of the differences from island to island[18,19], and as a result, the dynamics of mantle geochemical cycling[11].

Hawai'i as the archetype of mantle plumes

Wilson[20] recognized that the source of oceanic island volcanoes such as Hawai'i was fixed in space relative to plate motions and, thus, that it must be ultimately deeper than the lithosphere and upper mantle involved in plate tectonics. Hawai'i is the archetypical example of intraplate volcanism[5]. It is the longest island chain on Earth, extending almost 6,000 km in length, and has been active for over 80 million years. The Hawaiian islands are surrounded by a 1,000-km-wide bathymetric swell, the Hawaiian swell, commonly associated with a sublithospheric hot buoyant mantle plume[1,2,21] that extends well into the lower mantle[4] and possibly to the CMB[22], although seismic resolution at this depth (~2,800 km) is problematic[23]. The Hawaiian mantle plume has the largest buoyancy flux of any plume[1,2,21] and has been the subject of a large number of geochemical, fluid-dynamical and geodynamical studies[21,24–29].

[1]Department of Earth and Ocean Sciences, University of British Columbia, 6339 Stores Road, Vancouver, British Columbia V6T1Z4, Canada. [2]Pacific Centre for Isotopic and Geochemical Research, University of British Columbia, 6339 Stores Road, Vancouver, British Columbia V6T1Z4, Canada. [3]Department of Geology and Geophysics, University of Hawai'i, Honolulu, Hawai'i 96822, USA. [4]Department of Geosciences, University of Massachusetts, Amherst, Massachusetts 01003, USA. e-mail: dweis@eos.ubc.ca

© 2011 Macmillan Publishers Limited. All rights reserved

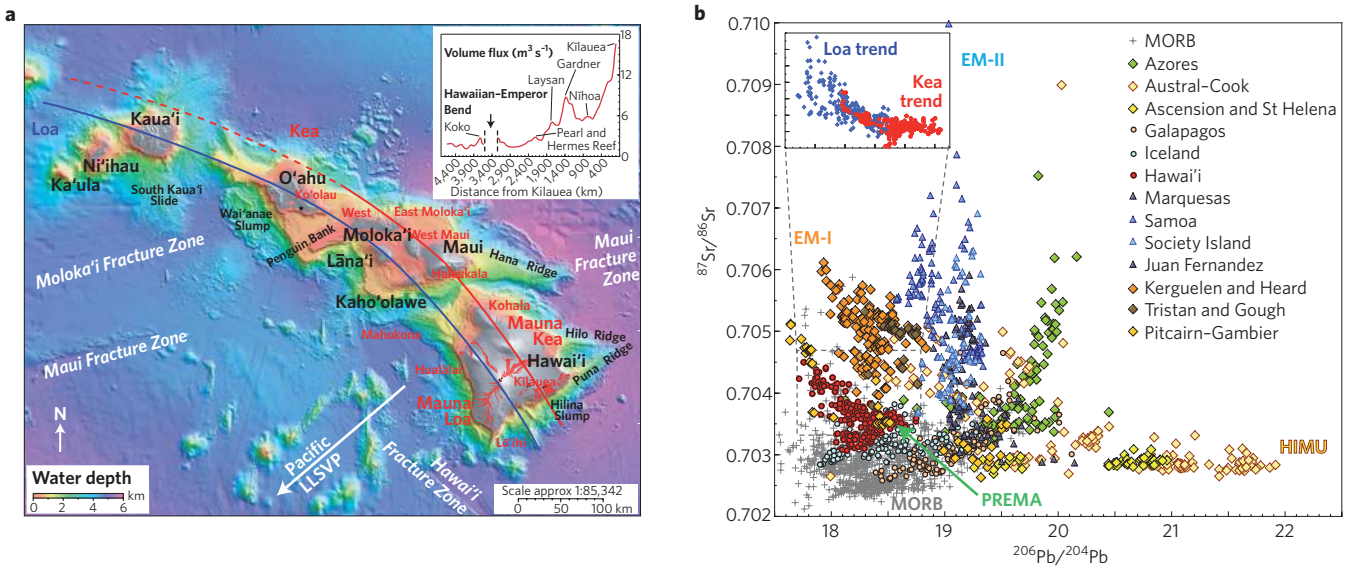

Figure 1 | Key bathymetric and isotopic features of the Hawaiian Islands. a, Bathymetric map (18° to 23°2′ N, 161° to 154° W) of the Hawaiian Islands[102]. The Loa and Kea trends are defined. Arrow points to the location of the Pacific LLSVP[66]. Temporal variation of volume flux of magma calculated assuming regional compensation[95] is shown in the inset. **b**, Sr–Pb isotope diagrams of oceanic basalts[103]. Inset shows recent data (including this study) on Hawaiian tholeiitic shield lavas. Kea volcanoes point towards average mantle compositions (PREMA[9]) and Loa volcanoes towards enriched compositions (EM-I type[9]).

The Hawaiian mantle plume was the target of a deep drilling study, the Hawai'i Scientific Drilling Project (HSDP), which provided a continuous sampling of ~3,255 m of the Mauna Kea volcano with ages between ~240 and >650 kyr (ref. 30), and represented a unique opportunity to study a significant portion of the life history of a plume-related volcano[7,31]. As Hawaiian volcanoes grow, they are slowly carried to the northwest by the moving Pacific plate at a speed of 9–10 cm per year[32], passing over the Hawaiian mantle plume. As the magma-producing region is roughly 100 km in diameter[21], the volcano takes about 1 million years to cross this region[33]. Numerous petrological and geochemical studies were carried out on the drill core samples to characterize the mantle source for the lavas and constrain the time-averaged rates of melt production, delivery to the crust and eruption at the surface. Together with results from complementary models of the Hawaiian plume, this combined effort represents a considerable leap forward in our understanding of plume-related volcanism in general[25,30,34–38].

During the past 5 Myr, Hawaiian volcanoes formed two parallel chains[39,40] (Fig. 1a) that are distinct geographically and geochemically[8]. These two chains, or Loa and Kea trends, are named after their tallest volcanoes, Mauna Loa and Mauna Kea, both on the Island of Hawai'i. High-precision lead isotope compositions show that there is little overlap between volcanoes from the two trends, with Loa-trend volcanoes characterized by higher $^{208}Pb/^{204}Pb$ for a given $^{206}Pb/^{204}Pb$ than Kea-trend volcanoes[27]. If the connection between mantle plume and hotspot is robust, these trends define azimuthally asymmetric compositional zoning in the plume conduit[26,29] that is difficult to reconcile with the popular concentrically zoned model of the mantle plume for Hawai'i[25,36,41].

The so-called bilateral compositional asymmetry of the Hawaiian mantle plume was initially defined on the basis of the Pb isotopic analyses of ~120 shield samples, dominantly from the Island of Hawai'i (Fig. 1a) for Kea-trend volcanoes (that is, Kīlauea, Mauna Kea and Kohala) and from 8–15 samples per volcano for Loa-trend volcanoes[27,35,42] (Lō'ihi, Mauna Loa, Lāna'i, Kaho'olawe and Ko'olau). Half of these samples were from the HSDP core from Mauna Kea volcano. Here we present new data on 120 Mauna Loa lavas, which are then integrated in a compilation of over 700 high-precision Pb isotopic compositions for shield-stage lavas from all the main islands of the chain (Fig. 2a and b), and also about 585 for Sr and Nd, and 485 samples for Hf isotopic compositions. All data for the different isotopic ratios have been normalized to the same standard values (see Supplementary Information for analytical techniques). The shield building phase represents ~98% of the volume of an average Hawaiian volcano[43]. The distinct Pb isotopic signatures of Loa- and Kea-trend volcanoes are clearly defined with only a few exceptions (29 out of 713 analysed samples, or 4% of the data set). Most of the distinctive samples have already been reported in the literature[27,35,44–48].

Isotopic study of the largest active volcano on Earth

Mauna Loa is the largest active volcano on the Earth, with a volume[49] of about 80,000 km³. Surprisingly, only a few studies have reported geochemical data on this volcano. In light of its significance in the Hawaiian chain, and the availability of new samples from both submarine and subaerial phases of volcano activity, we selected 120 new samples for this study (Fig. 3 and Supplementary Fig. S1, Table S1), covering: (1) a 1.6-km-thick submarine landslide section, called the Mile High Section, that allows continuous stratigraphic sampling analogous to HSDP[50] with ages between 120 and 470 kyr (ref. 51); (2) submersible and dredged samples along the submarine southwest rift zone; (3) radial vents on the southwest part of the Big Island[52]; (4) subaerial prehistoric and historic lavas[53]; and (5) a few samples from the 245 m of Mauna Loa recovered in the HSDP-2 core. A brief description of the sample location and geological context is given in the Supplementary Information. Combined with recently published isotopic data from Mauna Loa samples[34,42,45], our results confirm that the compositions of Mauna Loa lavas are distinct from those of Mauna Kea lavas. Mauna Loa tholeiitic basalts have $^{206}Pb/^{204}Pb$ between 18.05 and 18.26, with three landslide samples extending the compositional range up to 18.40, which is within the range of values for Lō'ihi[27]. There is no overlap in $^{206}Pb/^{204}Pb$ between Mauna Loa (<18.26) and Mauna Kea (>18.4) lavas. In a Pb–Pb isotope diagram (Fig. 2a), the analyses for the lavas are distributed systematically on either side of the Kea–Loa

© 2011 Macmillan Publishers Limited. All rights reserved

boundary, with only three prehistoric Mauna Loa samples crossing this boundary[45].

Among the 120 Mauna Loa samples analysed here, some of the older samples (~470 kyr)[51], collected at the lower levels of the landslide section on the submarine southwest rift zone, show different isotopic signatures, not observed anywhere else in Hawai'i (see Fig. 2b inset and Supplementary Fig. S1). These samples have higher $^{208}Pb/^{204}Pb$ for a given $^{206}Pb/^{204}Pb$ and lower $^{143}Nd/^{144}Nd$ for a given $^{87}Sr/^{86}Sr$. These signatures document the presence of more heterogeneities in the Loa source, especially in the earlier shield-building stage, than in the Kea source.

The difference between Loa- and Kea-trend volcanoes is best seen using $^{208}Pb^*/^{206}Pb^*$ (ref. 32), which is a measure of the radiogenic addition to $^{208}Pb/^{204}Pb$ and $^{206}Pb/^{204}Pb$ during the Earth's history and is calculated by subtracting the primordial (initial) isotope ratios from the measured values: $^{208}Pb^*/^{206}Pb^*$ reflects the ratio of Th/U integrated over the history of the Earth. Loa-trend volcanoes have $^{208}Pb^*/^{206}Pb^*$ values above 0.9475, whereas Kea-trend volcanoes have lower values (Figs 2b, 4b). In addition, Loa-trend volcanoes show a wider range of variations in all isotopic systems by a factor of about 1.5. For example, $^{206}Pb/^{204}Pb$ varies from 17.8 (West Ka'ena)[54] to 18.5 (Lō'ihi)[27], whereas Kea-trend volcanoes range from 18.2 (Kohala)[27] to 18.74 (Hilina)[55]. Similarly, ε_{Nd}, a measure of the deviation of $^{143}Nd/^{144}Nd$ from the chondritic value ($^{143}Nd/^{144}Nd = 0.512638$), varies about twice as much in Loa-trend volcanoes (from −0.9 to +7.5, Ko'olau)[48] than in Kea-trend volcanoes (from +5.1 in Haleakalā[56] to +8.2 in West Maui[57]). There is limited overlap between the two trends in isotopic signatures. The range of variations is larger in Loa-trend volcanoes, as expressed by two standard deviations on the average of isotopic analyses of lavas of each individual volcano, and increases with increasing age along the Hawaiian chain (that is, farther away from Kīlauea; Fig. 4a and b).

Kea-trend volcanoes define Pb–Pb isotope mixing arrays (Fig. 2a, inset) that converge towards radiogenic Pb ratios ($^{206}Pb/^{204}Pb = ~18.5–18.6$, $^{208}Pb/^{204}Pb = ~38.1–38.2$), which Tanaka *et al.*[48] called the Kea component. A few of the Kea volcano arrays cross the Kea–Loa boundary, indicating that one of the least radiogenic endmembers of the Kea volcanoes belongs to the Loa compositional field. In contrast, the Loa-trend volcanoes define Pb–Pb mixing arrays (Fig. 2a, inset) that are mostly subparallel to the Kea–Loa boundary and that rotate slightly around a common point close to Mauna Loa average compositions ($^{206}Pb/^{204}Pb = ~18.1–18.2$, $^{208}Pb/^{204}Pb = ~37.9$), which shows that this is a prevalent composition on the Loa side of the boundary. A few older Loa-trend volcanoes (Lāna'i, Ko'olau Makapu'u stage, Kaho'olawe) define Pb–Pb mixing arrays with either steeper or shallower slopes. These arrays intersect close to the average composition of the enriched Hawai'i endmember, the enriched Makapu'u component (EMK) of Tanaka *et al.*[48], that is interpreted to reflect the presence of recycled oceanic crust and sediments[58]. The different organization of Pb–Pb isotope mixing arrays for Loa- and Kea-trend volcanoes indicates the presence of distinct endmember compositions in the source of the two geographic trends of Hawaiian volcanoes.

The geochemical differences between the Loa- and Kea-trend volcanoes probably reflects compositional variations in the plume source region at or near the CMB. These differences have persisted for at least 5 million years[54,59] and are not related to temporal variations in the degree of melting, although we do not yet know when the Loa and Kea trends emerged in the volcanic record at the surface. Below we examine what the geochemical differences between the Loa and Kea trends imply in terms of the bulk composition and structure of the deep source of the plume.

Geochemical trends linked with deep mantle structure

The source region for the Hawaiian plume is widely recognized to be complex in structure, physical properties, constitution and composition[60]. Inferences from recent seismological studies[61], together with

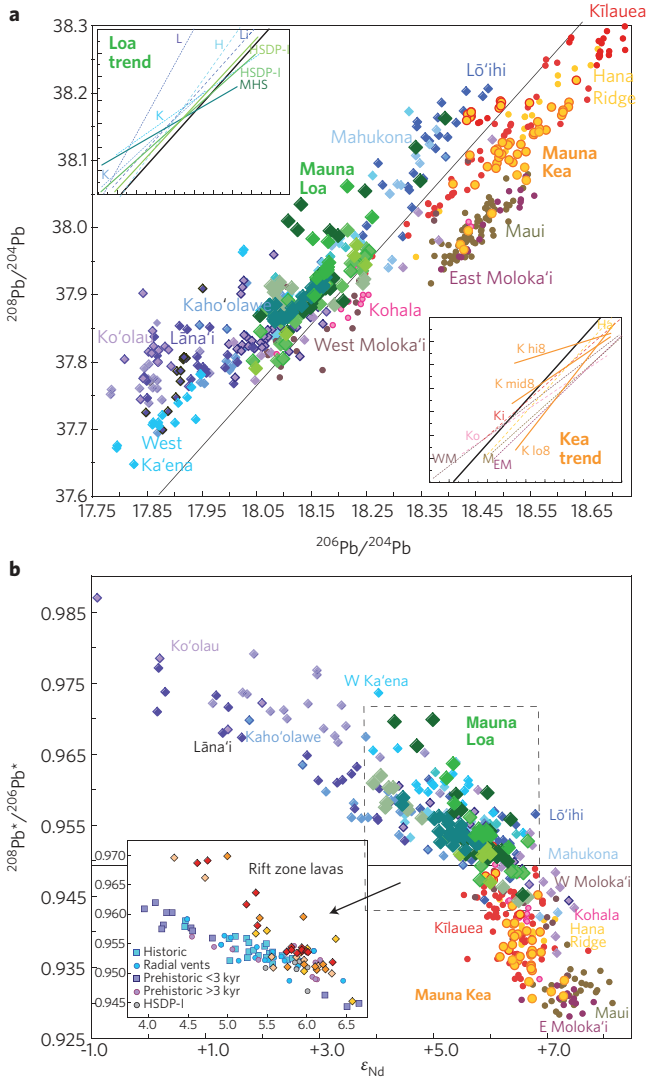

Figure 2 | Isotopic data for Hawaiian shield lavas. a, Plot of $^{208}Pb/^{204}Pb$ against $^{206}Pb/^{204}Pb$ for all Hawaiian shield lavas (normalized to same standard values). Mauna Loa and Mauna Kea samples have larger symbols. Thick black line indicates boundary separating volcanoes on the Mauna Loa (diamonds and cool colours) and Mauna Kea (circles and warm colours) trends based on Pb isotopic composition[27]. Insets: Pb–Pb arrays among some of the individual volcanoes. Solid lines indicate Mauna Loa (HSDP-I and Mile High Section, MHS) and Mauna Kea (low-, mid- and high-8)[35]. Dashed lines indicate other Hawaiian volcanoes or features (Li, Lō'ihi; H, Hualālai; L, Lāna'i; K, Kaho'olawe; Ha, Hana Ridge; Ki, Kīlauea; Ko, Kohala; M, Maui; EM, East Moloka'i; WM, West Moloka'i). **b,** Plot of $^{208}Pb^*/^{206}Pb^*$ against ε_{Nd} for Hawaiian shield lavas. Inset: plot of $^{208}Pb^*/^{206}Pb^*$ against ε_{Nd} detail of Mauna Loa lavas (this study, plus prehistoric lavas <3 kyr old[45], radial vents[52]), where older samples (red, yellow and orange diamonds; see also Supplementary Fig. S1) sampled along the submarine southwest rift zone define a unique mixing trend. Darker outline indicates triple-spike literature data. See Supplementary Information for all data sources.

© 2011 Macmillan Publishers Limited. All rights reserved

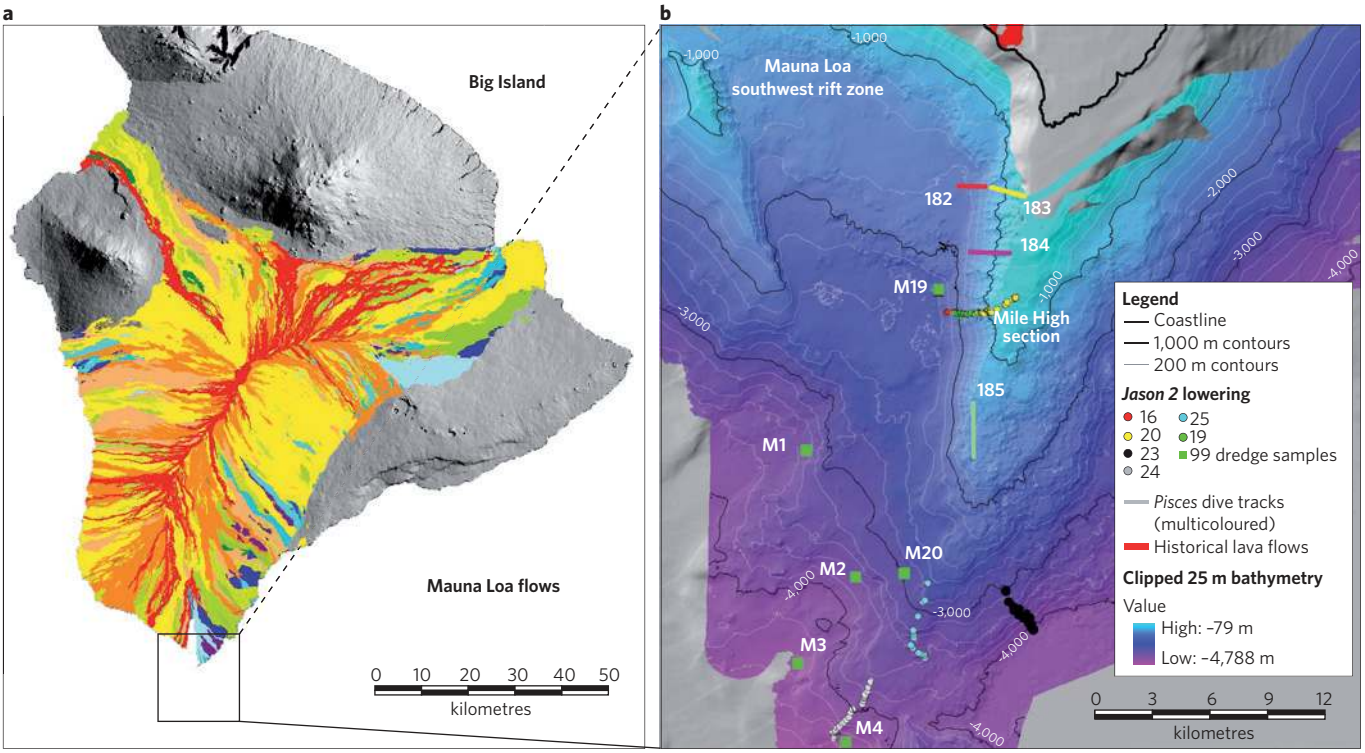

Figure 3 | Mauna Loa flows and southwest submarine rift zone. a,Topographic shaded relief map of the Big Island of Hawai'i, highlighting Mauna Loa flows[104]. Flow colours indicate relative age (red, young; blue, old). Inset, area of Fig. 3b. **b,** Bathymetric map of the Mauna Loa submarine southwest rift zone showing the dredge and dive locations, and the Mile High Section sampled by the ROV *Jason 2* and *Pisces 5* dives. Contours from UTM Zone 5 NAD27, bathymetric map produced by G. Kaye, USGS-HVO, from data collected on the Mauna Loa HUGO (Hawai'i Undersea Geo-Observatory) oceanographic cruise (2002).

kinematic mantle flow models[62], show that the location of Hawai'i, when projected down to the CMB region, overlies the northeastern edge of the 'large low-shear-velocity province' (LLSVP)[63–65] in the Pacific Ocean (Fig. 5c, adapted from ref. 66). The province is an anomalously dense, compositionally distinct[67] region, steep-sided and several hundred kilometres high. The Loa and Kea volcanoes straddle the LLSVP boundary with the Loa side of the Hawaiian plume located above the LLSVP and the Kea side overlying average Pacific lower mantle. One explanation for the distinct geochemical character of the Loa and Kea trends (Fig. 5b) is that they continuously sample these two qualitatively different types of mantle. This implies that the LLSVP mantle is, on average, more enriched in incompatible elements and more variable isotopically, whereas the Pacific lower mantle, preferentially sampled by the Kea side, is less heterogeneous.

Such a long-term physical link between the isotopic composition of the basalts and the source region requires that the root Hawaiian plume has remained approximately fixed at the edge of the LLSVP, and that there is little internal lateral or azimuthal stirring within the overlying the plume conduit. Steep-sided LLSVP piles, if over 50 km high, will introduce lateral temperature variations capable of driving an upward flow that will ultimately anchor the Hawaiian plume conduit[6]. The fixity of the plume to a LLSVP pile is therefore to be expected. The preservation of the spatially and chemically distinct Loa and Kea heterogeneities is perhaps surprising because the Hawaiian plume is strongly tilted[62,68,69]. Although lateral temperature variations can drive convection around the edges of a tilted conduit[70], causing internal azimuthal stirring, as well as the entrainment and mixing of surrounding mantle across the conduit, such a process is negligible for the range of plume strength and plate flow conditions expected for the Earth[26,71]. Indeed, even strongly tilted plumes will preserve the essential heterogeneous structure of their source region. The geometry and distribution of heterogeneities in the source region of the Hawaiian plume determine what is delivered to the melting region and sampled by the volcanoes[29]. An alternative view is that broadly concentric zoning of the plume is expected and that, at any given depth within the plume conduit, lateral mixing will result from the rheological variability across the plume conduit[72]. The extensive data set of new and published isotopic analyses presented here, on more than 700 Hawaiian basalt samples, shows the presence of two trends for at least 5 Myr from the Island of Hawai'i to Kaua'i with no evidence for concentric zoning.

If the variation in Pb isotopes in Loa basalts is related to entrainment of LLSVP mantle, then the heterogeneities may initially have a relatively low viscosity[6]. A low-viscosity tendril will be sheared at a greater rate and to a greater extent than the surrounding plume material in the conduit, giving rise to shear instabilities that could lead to entrainment and mixing across the conduit[73]. Such viscosity interfaces are never stable[74], but the timescale for the growth of this instability is much longer than the time for plume material to rise across the mantle depth. Thus, the presence of such viscosity variations will probably not lead to lateral mixing and alter significantly our proposed connection between Hawaiian basalts and the composition of the source region.

From recent seismic imaging using scattered waves[75], it has been inferred that the Hawaiian plume material ponds in the transition zone before travelling more than 1000 km east to Hawai'i. This study concludes that the hotspot is consequently decoupled from the source region and that isotope signatures of surface lavas cannot be used to map geochemical domains in the lower mantle. Partial ponding of rising plume material within the transition zone is, however, expected[76,77]. A stabilizing buoyancy effect and cooling related to the endothermic post-spinel phase transition at ~670 km will cause

© 2011 Macmillan Publishers Limited. All rights reserved

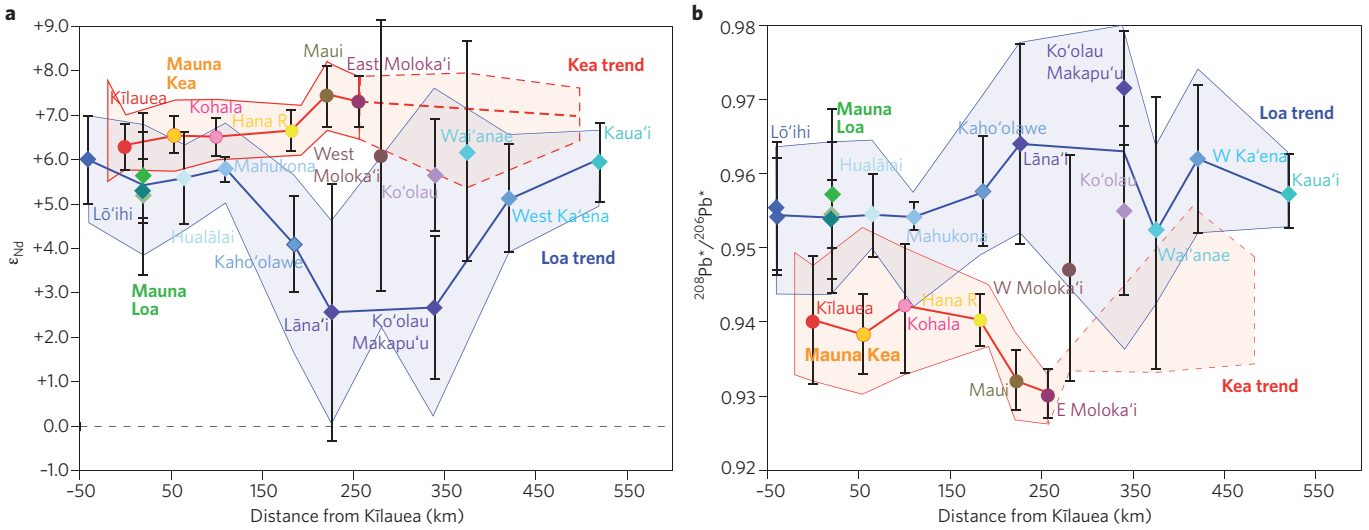

Figure 4 | Temporal evolution of isotopic compositions from Hawaiian volcanoes. a, Plot of ε_{Nd} against distance from Kīlauea in kilometres along the Hawaiian chain. **b**, Plot of $^{208}Pb^*/^{206}Pb^*$ against distance from Kīlauea. Symbols, colour coding and data source (plus Wai'anae) as in Fig. 2. See Supplementary Information for data sources. Individual volcanoes are represented by the average of the analyses of shield lavas (thermal ionization triple-spike or multicollector inductively coupled plasma mass spectrometry data), with the two standard deviation on the mean used to indicate the variation around the average. Shaded fields indicate the total range of variation covered for each volcano.

plume material rising across this phase transition to slow down and the conduit to spread out to conserve mass. Ponding in the transition zone is, however, not consistent with body-wave studies based on an extensive regional network of ocean bottom seismometers network which identified a deep-seated low-velocity anomaly under Hawai'i and a deep source for the Hawaiian mantle plume[22,69,78].

The crucial issue for the link between the Loa and Kea basalt compositions and their source regions is whether this spreading would introduce motions that stir the heterogeneities carrying the trends together or cause significant entrainment of ambient mantle material that would ultimately overwhelm the signal from the deep mantle source. Whereas the effects of phase transitions on the rise of starting plume head, and thus the composition of flood basalts, have received significant attention[79,80], the effect on plume tails is less certain. However, the spreading of the conduit as a gravity current involves only an additional component of pure shear[81] that will widen the Loa and Kea anomalies, but will not cause them to mix.

Finally, it is still unclear at this stage if the partial ponding of plume material modelled in the transition zone 1,000 km west of Hawai'i[75] is indeed linked to the Hawaiian mantle plume, and, if so, what the physical link is with the volcanic activity observed on the Hawaiian Islands. Indeed, it would imply a transfer of material in the opposite direction to the mantle wind in the Pacific[82] (in the direction of the Pacific plate motion, towards the northwest) for over 80 Myr.

Loa component and fine-scale structure of LLSVP

The greater isotopic and geochemical variability of the Loa volcanoes is a remarkable feature that, in principle, requires that the source of the Loa side of the plume is compositionally heterogeneous over many length scales, consistent with recent seismological studies[63,83,84]. A plausible source for some of this additional heterogeneity is a thin (5–50 km) ultra-low-seismic-velocity zone (ULVZ) lens, where P- and S-wave velocities are reduced by up to 10% and 30%, respectively[60,85], concentrated near the edge of the LLSVP pile[66,85,86] beneath the Loa side of Hawai'i. These structures have recently been modelled as regions of dense[87,88] partial melt, presumably enriched in incompatible elements, which is variably stirred, depending on the competition between compaction and melt drainage and melt retention as a result of coupling to overlying mantle flow[87,89].

Our model assumes that the Loa- and Kea-trend compositions and the heterogeneity spectrum for Hawaiian basalts are preserved through the melt extraction process. We assume that there is negligible mechanical mixing of melts between the melting region and the surface. In Iceland, where the mantle plume coincides with the Mid-Atlantic Ridge, mixing has been proposed to explain the spectrum of Pb isotope variability in olivine-hosted melt inclusions, at the 100- to 500-μm scale[90]. The existence of individual Pb–Pb arrays for each Hawaiian volcano indicates that mixing occurs at the scale of the plume conduit, 10–50 km (refs 34, 45). Most recent melt extraction models[91] suggest that compaction draws melts together over length scales of at most a few kilometres or a few per cent of the width of the melting region[29]. Thus, whereas this effect may smooth out the spatial variability within each trend as it is expressed at the surface, it is unlikely to affect the qualitative differences between the Loa and Kea endmembers as reflected by the existence of the two parallel chains of volcanoes with distinct geochemical signatures for at least 5 Myr.

Comparisons with other ocean islands

The geochemistry of the Loa-trend volcanoes (higher Th/U, as indicated by their higher $^{208}Pb^*/^{206}Pb^*$, lower ε_{Nd} and ε_{Hf} and higher $^{87}Sr/^{86}Sr$ compared with Kea-trend volcanoes) indicates the presence of an enriched component, most prevalent in Lāna'i and Ko'olau volcanoes[27,48]. These geochemical characteristics require a source more enriched in incompatible elements for Loa-trend volcanoes than for those on the Kea trend, and these features could correspond to the ULVZ, which is chemically distinct and probably partially molten[85,92].

There continues to be debate about the shape, origin and composition of the LLSVP and ULVZ[60,66], as well as on the role of core–mantle interaction[93] in the generation of heterogeneities in the Earth's mantle. Several authors argue for contribution from the core, on the basis of coupled enrichments in $^{186}Os/^{188}Os$ and $^{187}Os/^{188}Os$ in plume-derived materials when compared with upper-mantle materials[93]. Assessing the geometry, physical structure and extent of ULVZ is still a challenge because of poor tomographic resolution at the CMB and the basic trade-off between velocity reduction and spatial size in forward models relying on seismic ray theory[66]. Materials that could be present in the lowermost mantle include partially molten residues of early Earth differentiation (4.5 billion years ago), subducted

© 2011 Macmillan Publishers Limited. All rights reserved

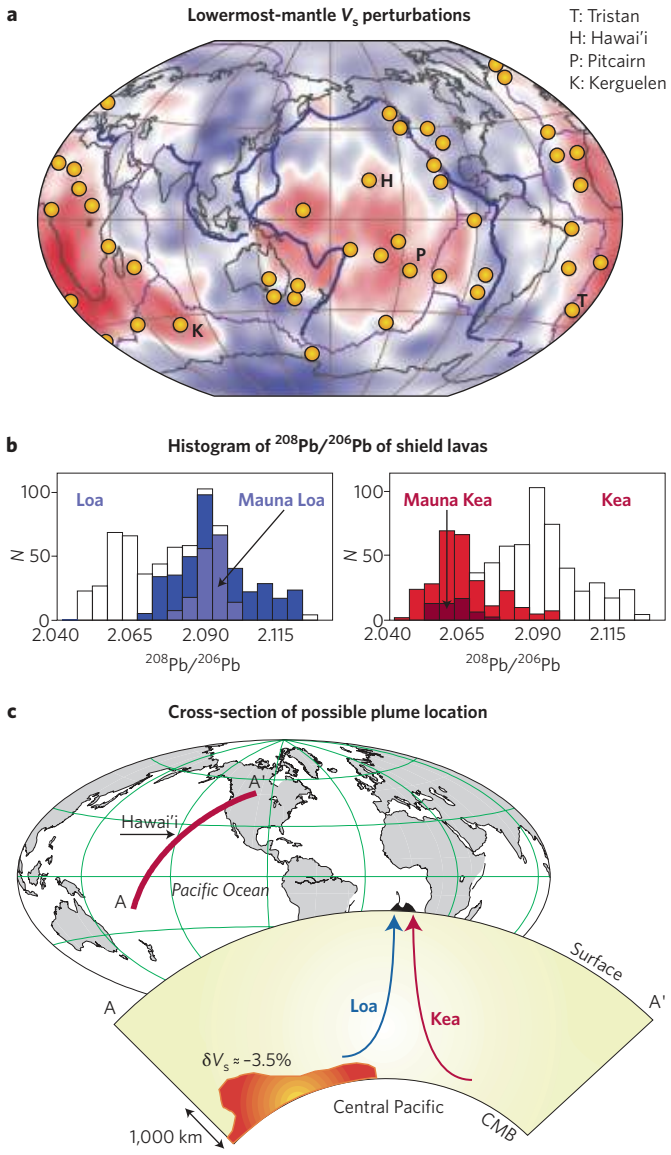

Figure 5 | Deep mantle velocity anomalies and hotspot locations. **a,** Global map showing the lowermost-mantle V_s perturbations from tomographic model TXBW[105] (adapted from ref. 66). Continents, thin black outline; Pacific 'Ring of Fire', thick blue line; circles, hotspot locations[106]. Red and blue colours indicate lower and higher velocities than global average, respectively. The peak-to-peak value for this model is 5.5. Hawai'i and Pitcairn (Pacific Ocean), Kerguelen (Indian Ocean) and Tristan (Atlantic Ocean) have EM-I-type geochemical signatures. **b**, Histogram of $^{208}Pb/^{206}Pb$ (used to minimize analytical noise on ^{204}Pb) for Hawaiian shield lavas. **c,** Cross-section through the Hawaiian mantle plume down to the CMB, showing a schematic representation of the low-velocity structures beneath the central Pacific (after ref. 107, modified after ref. 66). Hawaiian Island surface locations and relative position of the Loa and Kea trends in the mantle plume are indicated.

slabs (heterogeneous mixture of sediments, altered oceanic crust and upper mantle), and metal from the outer core (see discussion in ref. 7)[11,12,18,19,83]. Recent $^{142}Nd/^{144}Nd$ studies of deeply sourced mantle plumes, including Hawai'i, present no evidence for the interaction with an early-enriched reservoir (EER) in the source of these basalts[94].

Loa-trend geochemical characteristics have persisted for at least ~5 million years[54,59]. This period had the highest magma production rate for the Hawaiian mantle plume (Fig. 1a, inset)[95]. The overall variability among the Loa volcanoes is time-dependent and seems to be larger in the older volcanoes (West Kaʻena, Koʻolau) than in recent ones (Lōʻihi) (Fig. 4a and b). The appearance of the Loa component is probably related to the sampling of the relatively dense, partially melted material in the anomalous velocity lenses at the CMB by the Hawaiian mantle plume and could coincide with elevated magma production rates[48].

Other surface hotspot locations can be correlated with lateral shear-wave (S-wave) velocity gradients in the deep mantle[61,96]. Kerguelen, another EM-I oceanic island with a strong enriched signature (Fig. 1b) in the Indian Ocean[97], is located on the eastern end of the tall steep-sided LLSVP African anomaly[98] (Fig. 5a). Tristan and Pitcairn are two other islands with EM-I signature (Fig. 1b)[18]. When projected onto the CMB, Tristan is located on the western border of the LLSVP African anomaly, whereas Pitcairn straddles a boundary zone in the Pacific LLSVP. We infer that these deep velocity anomalies at the CMB are the repositories for enriched components in the mantle and are brought to the surface by strong mantle plumes. Above the Pacific LLSVP, Pitcairn and Hawai'i carry an enriched signature that is slightly less pronounced and distinct from the one carried by Kerguelen and Tristan, the 'DUPAL anomaly'[99,100], above the African LLSVP (Fig. 1b). These differences in EM-1 compositions correspond to differences in the sources of these islands and indicate that the material constituting the LLSVP at the base of the CMB is different in the Pacific and African anomalies.

Longevity of Loa component and Pacific LLSVP

To explore more fully the implications of our proposal that the Hawaiian mantle plume provides a long-lived probe of the composition and structure of its CMB source region, and that the LLSVP and ULVZ are repositories of enriched mantle components related either to the early differentiation of the Earth[14,15] or to the presence of subducted material[11,12,18], we need to go further back in time. High-precision isotopic studies of Hawai'i volcanoes have only been undertaken for lavas erupted during the last 5 Myr and for the Emperor Seamounts (85–42 Myr ago). Thus, our study of the Hawai'i volcanoes provides only a recent snapshot of the situation. There seem to be distinct differences between the Emperor (85 to 42 Myr ago) and Hawaiian (41 Myr ago to present) parts of the Hawaiian–Emperor Chain. In particular, Emperor-chain basalts have Kea-only compositions and were erupted at an approximately constant rate[48,95,101]. In contrast the 5-million-year record of volcanism at Hawai'i is characterized by this remarkable Kea–Loa compositional asymmetry and a magma production rate that has increased greatly over time (Fig. 1a, inset)[95].

The appearance of the Loa composition may coincide with an increase in magma supply that is evident in the larger size of the Hawaiian volcanoes over the past 5 million years. Alternatively, Loa composition may extend back to the prominent bend in the Hawaiian–Emperor Chain. This dichotomy in isotopic composition and increase in eruption rate could ultimately be linked to changes in the thickness, thermal structure[23] and dynamics of the LLSVP part of the plume source region in the deep mantle.

In principle, the Hawaiian–Emperor hotspot track in the Pacific Ocean with 85 million years of activity (and the Kerguelen hotspot track in the Indian Ocean with an even longer 115 million years of activity) can provide unique insights into our proposed relationship between basalt composition and deep mantle structure. To fingerprint the changes in the source composition over the eruption time series recorded by the Hawaiian chain and to assess when the Loa component appeared will require additional high-precision isotopic work on the remaining 3,400 km of the chain to the northwest of the island of Kauaʻi. The timing of the segregation of the LLSVP in the lower mantle and the conditions of its sampling by the Hawaiian mantle plume are two issues that cannot yet be solved. Additional

© 2011 Macmillan Publishers Limited. All rights reserved

complementary high-resolution seismological studies of this part of the CMB region will be crucial to make links between the evolving composition of the source region and its structure and constitution. Resolving these fundamental issues will require increased collaboration among disciplines studying the Earth's deep interior.

References

1. Davies, G. F. Role of the lithosphere in mantle convection. *J. Geophys. Res.* **93,** 10451–10466 (1988).
2. Sleep, N. Hotspots and mantle plumes: Some phenomenology. *J. Geophys. Res.* **95,** 6715–6736 (1990).
3. Richards, M. A., Duncan, R. A. & Courtillot, V. E. Flood basalts and hot-spot tracks: Plume heads and tails. *Science* **246,** 103–107 (1989).
4. Montelli, R., Nolet, G., Dahlen, F. A. & Masters, G. A catalogue of deep mantle plumes: New results from finite-frequency tomography. *Geochem. Geophys. Geosyst.* **7**, Q11007 (2006).
5. Morgan, W. J. Convection plumes in the lower mantle. *Nature* **230,** 42–43 (1971).
6. Jellinek, A. & Manga, M. Links between long-lived hot spots, mantle plumes, D" and plate tectonics. *Rev. Geophys.* **42**, RG3002 (2004).
7. DePaolo, D. J. & Weis, D. in *Continental Scientific Drilling: A Decade of Progress, and Challenges for the Future* (eds Harms, U., Koeberl, C. & Zoback, M. D.), Springer, pp. 259–288 (2007).
8. Tatsumoto, M. Isotopic composition of lead in oceanic basalt and its implication to mantle evolution. *Earth Planet. Sci. Lett.* **38,** 63–87 (1978).
9. Zindler, A. & Hart, S. Chemical geodynamics. *Annu. Rev. Earth Planet. Sci.* **14,** 493–571 (1986).
10. Sun, S. & McDonough, W. Chemical and isotopic systematics of oceanic basalts: Implications for mantle composition and processes, in *Magmatism in the Ocean Basins* (eds Saunders, A. D. & Norry, M. J.) *Geol. Soc. London Spec. Publ.* **42,** 313–345 (1989).
11. Hofmann, A. W. in *The Mantle and the Core* (ed. Carlson, R. W.), *Treatise of Geochemistry* Vol. 2 (eds. Holland H. D. & Turekian K. K.), 61–101 (Elsevier–Pergamon, 2003).
12. White, W. Oceanic island basalts and mantle plumes: the geochemical perspective. *Annu. Rev. Earth Planet. Sci.* **38,** 133–160 (2010).
13. White, W. M. Sources of oceanic basalts — radiogenic isotopic evidence. *Geology* **13,** 115–118 (1985).
14. Labrosse, S., Hernlund, J. W. & Coltice, N. A crystallizing dense magma ocean at the base of the Earth's mantle. *Nature* **450,** 866–869 (2007).
15. Carlson, R. W., Boyet, M. Composition of the Earth's interior: the importance of early events. *Phil. Trans. R. Soc. A* **366,** 4077–4103 (2008).
16. van Keken, P., Hauri, E. H. & Ballentine, C. J. Mantle mixing: The generation, preservation, and destruction of chemical heterogeneity. *Annu. Rev. Earth Planet. Sci.* **30,** 493–525 (2002).
17. Albarède, F. & van der Hilst, R. Zoned mantle convection. *Phil. Trans. R. Soc. A* **360,** 2569–2592 (2002).
18. Willbold, M. & Stracke, A. Trace element composition of mantle end-members: Implications for recycling of oceanic and upper and lower continental crust. *Geochem. Geophys. Geosyst.* **7**, Q04004 (2006).
19. Willbold, M. & Stracke, A. Formation of enriched mantle components by recycling of upper and lower continental crust. *Chem. Geol.* **276,** 188–197 (2010).
20. Wilson, J. T. Evidence from islands on the spreading of the ocean floor. *Can. J. Phys.* **41,** 863–868 (1963).
21. Ribe, N. & Christensen, U. The dynamical origin of Hawaiian volcanism. *Earth Planet. Sci. Lett.* **171,** 517–531(1999).
22. Wolfe, C. J. *et al.* Mantle shear-wave velocity structure beneath the Hawaiian hot spot. *Science* **326,** 1388–1390 (2009).
23. Lenardic, A. & Jellinek, A. M. Tails of two plume types in one mantle. *Geology* **37,** 127–130 (2009).
24. Richards, M. A. & Griffiths, R. W. Deflection of plumes by mantle shear flow: experimental results and a simple theory. *Geophys. J.* **94,** 367–376 (1988).
25. DePaolo, D. J., Bryce, J., Dodson, A., Shuster, D. & Kennedy, B. Isotopic evolution of Mauna Loa and the chemical structure of the Hawaiian plume. *Geochem. Geophys. Geosyst.* **2,** 1044 (2001).
26. Kerr, R. & Mériaux, C. Structure and dynamics of sheared mantle plumes. *Geochem. Geophys. Geosyst.* **5**, Q12009 (2004).
27. Abouchami, W. *et al*. Lead isotopes reveal bilateral asymmetry and vertical continuity in the Hawaiian mantle plume. *Nature* **434,** 851–856 (2005).
28. Ren, Z., Ingle, S., Takahashi, E., Hirano, N. & Hirata, T. The chemical structure of the Hawaiian mantle plume. *Nature* **436,** 837–840 (2005).
29. Farnetani, C. G. & Hofmann, A. W. Dynamics and internal structure of the Hawaiian plume. *Earth Planet. Sci. Lett.* **295,** 231–240 (2010).
30. Sharp, W. & Renne, P. The $^{40}Ar/^{39}Ar$ dating of core recovered by the Hawaii Scientific Drilling Project (phase 2), Hilo, Hawaii. *Geochem. Geophys. Geosyst.* **6**, Q04G17 (2005).
31. Stolper, E. M., DePaolo, D. J. & Thomas, D. M. Deep drilling into a mantle plume volcano: the Hawaii Scientific Drilling Project. *Scient. Drilling* **7,** 4–14 (2009).
32. Clague D. A., Dalrymple G. B. The Hawaiian–Emperor volcanic chain Part 1. Geologic evolution. *USGS Prof. Pap.* **1350,** 5–54 (1987).
33. Garcia, M. O., Caplan-Auerbach, J., De Carlo, E. H., Kurz. M. D. & Becker, N., Geology, geochemistry and earthquake history of Loihi seamount, Hawaii's youngest volcano. *Chem. Erde* **66,** 81–108 (2006).
34. Blichert-Toft, J., Weis, D., Maerschalk, C., Agranier, A. & Albarède, F. Hawaiian hot spot dynamics as inferred from the Hf and Pb isotope evolution of Mauna Kea volcano. *Geochem. Geophys. Geosyst.* **4,** 8704 (2003).
35. Eisele, J., Abouchami, W., Galer, S. J. G. & Hofmann, A. W. The 320 kyr Pb isotope evolution of Mauna Kea lavas recorded in the HSDP-2 drill core. *Geochem. Geophys. Geosyst.* **4,** 8710 (2003).
36. Kurz, M., Curtice, J., Lott, D. & Solow, A. Rapid helium isotopic variability in Mauna Kea shield lavas from the Hawaiian Scientific Drilling Project. *Geochem. Geophys. Geosyst.* **5**, Q04G14 (2004).
37. Rhodes, J. M. & Vollinger, M. J. Composition of basaltic lavas sampled by phase-2 of the Hawaii Scientific Drilling Project: Geochemical stratigraphy and magma types, *Geochem. Geophys. Geosyst.* **5**, Q03G13 (2004).
38. Bryce, J., DePaolo, D. J. & Lassiter, J. Geochemical structure of the Hawaiian plume: Sr, Nd, and Os isotopes in the 2.8 km HSDP-2 section of Mauna Kea volcano. *Geochem. Geophys. Geosyst.* **6**, Q09G18 (2005).
39. Dana, D. J. *Geology, Report of the United States Exploring Expedition, 1838–1842*, Vol. 10 (C. Sherman, Philadelphia, 1849).
40. Jackson, E. D., Shaw, H. R. & Bargar, K. E. Calculated geochronology and stress field orientations along the Hawaiian chain. *Earth Planet. Sci. Lett.* **26,** 145–155 (1975).
41. Lassiter, J., DePaolo, D. J. & Tatsumoto, M. Isotopic evolution of Mauna Kea volcano: Results from the initial phase of the Hawaii Scientific Drilling Project. *J. Geophys. Res.* **101,** 11769–11780 (1996).
42. Abouchami, W., Galer, S. J. G. & Hofmann, A. W. High precision lead isotope systematics of lavas from the Hawaiian Scientific Drilling Project. *Chem. Geol.* **169,** 187–209 (2000).
43. Clague, D. A. Hawaiian alkaline volcanism. *Geol. Soc. London Spec. Pub.* **30,** 227–252 (1987).
44. Ren, Z.-Y., Tomoyuki, S., Masako, Y., Johnson, K. M. & Takahashi, E. Isotope compositions of submarine Hana Ridge lavas, Haleakala volcano, Hawaii: Implications for source compositions melting process and the structure of the Hawaiian plume. *J. Petrol.* **47,** 255–275 (2006).
45. Marske, J. P., Pietruszka, A. J., Weis, D., Garcia, M. O. & Rhodes, J. M. Rapid passage of a small-scale mantle heterogeneity through the melting regions of Kilauea and Mauna Loa Volcanoes. *Earth Planet. Sci. Lett.* **259,** 34–50 (2007).
46. Hanano, D., Weis, D., Scoates, J. S., Aciego, S. & DePaolo, D. J. Horizontal and vertical zoning of heterogeneities in the Hawaiian mantle plume from the geochemistry of consecutive postshield volcano pairs: Kohala-Mahukona and Mauna Kea-Hualalai. *Geochem. Geophys. Geosyst.* **11**, Q01004 (2010).
47. Xu, G. *et al.* Geochemical characteristics of West Molokai shield- and postshield-stage lavas: Constraints on Hawaiian plume models. *Geochem. Geophys. Geosyst.* **8,** Q08G21 (2007).
48. Tanaka, R., Makishima, A. & Nakamura, E. Hawaiian double volcanic chain triggered by an episodic involvement of recycled material: Constraints from temporal Sr-Nd–Hf–Pb isotopic trend of the Loa-type volcanoes. *Earth Planet. Sci. Lett.* **265,** 450–465 (2008).
49. Robinson, J. & Eakins, B. Calculated volumes of individual shield volcanoes at the young end of the Hawaiian Ridge. *J. Volcanol. Geotherm. Res.* **151,** 309–317 (2006).
50. Garcia, M. O., Hulsebosch, T. P. & Rhodes, J. M. in *Mauna Loa Revealed: Structure, Composition, History, and Hazards* (eds. Rhodes, J. M. & Lockwood, J. P.), *Geophys. Monogr. Ser.* **92**. American Geophysical Union, Washington, DC, pp. 219–239 (1995).
51. Jicha, B., Rhodes, J. M., Singer, B. S., Vollinger, M. J., Garcia, M. O. $^{40}Ar/^{39}Ar$ geochronology of submarine Mauna Loa volcano, Hawaii. American Geophysical Union, Fall Meeting, abstract #V43F-2328 (2009).
52. Wanless, V. D. *et al.* Submarine radial vents on Mauna Loa Volcano, Hawaii. *Geochem. Geophys. Geosyst.* **7**, Q05001 (2006).
53. Rhodes, J. M. & Hart, S. R. in *Mauna Loa Revealed: Structure, Composition, History, and Hazards* (eds Rhodes, J. M. & Lockwood, J. P.), *Geophys. Monogr. Ser.* **92**. 263–288 (American Geophysical Union, 1995).
54. Greene, A. R. *et al.* Low-productivity Hawaiian volcanism between Kaua'i and O'ahu. *Geochem. Geophys. Geosyst.* **11**, Q0AC08 (2010).
55. Kimura, J., Sisson, T., Nakano, N., Coombs, M. & Lipman, P. Isotope geochemistry of early Kilauea magmas from the submarine Hilina bench: The nature of the Hilina mantle component. *J. Volcanol. Geotherm. Res.* **151,** 51–72 (2006).
56. Chen, C., Frey, F. A., Garcia, M. O., Dalrymple, G. & Hart, S. R. The tholeiite to alkalic basalt transition at Haleakala Volcano, Maui, Hawaii. *Contrib. Mineral. Petrol.* **106,** 183–200 (1991).
57. Gaffney, A., Nelson, B. & Blichert-Toft, J. Geochemical constraints on the role of oceanic lithosphere in intra-volcano heterogeneity at West Maui, Hawaii. *J. Petrol.* **45,** 1663–1687 (2004).
58. Blichert-Toft, J., Frey, F. A. & Albarède, F. Hf isotope evidence for pelagic sediments in the source of Hawaiian basalts. *Science* **285,** 879–882 (1999).

© 2011 Macmillan Publishers Limited. All rights reserved

59. Garcia, M. O. *et al.* Petrology, geochemistry and geochronology of Kaua'i lavas over 4.5 Myr: implications for the origin of rejuvenated volcanism and the evolution of the Hawaiian plume. *J. Petrol.* **51,** 1507–1540 (2010).
60. Garnero, E. J. & McNamara, A. Structure and dynamics of Earth's lower mantle. *Science* **320,** 626–628 (2008).
61. Thorne, M., Grand, S. & Garnero, E. Geographic correlation between hot spots and deep mantle lateral shear-wave velocity gradients. *Phys. Earth Planet. Inter.* **176,** 47–63 (2004).
62. Burke, K., Steinberger, B., Torsvik, T. H. & Smethurst, M. A. Plume generation zones at the margins of large low shear velocity provinces on the core–mantle boundary. *Earth Planet. Sci. Lett.* **265,** 49–60 (2008).
63. Ritsema, J., van Heijst, H. & Woodhouse, J. Complex shear wave velocity structure imaged beneath Africa and Iceland. *Science* **286,** 1925–1928 (1999).
64. Mégnin, C. & Romanowicz, B. The shear velocity structure of the mantle from the inversion of body, surface, and higher modes waveforms. *Geophys. J. Int.* **143,** 709–728 (2000).
65. To, A., Fukao, Y. & Tsuboi, S. Evidence for a thick and localized ultra low shear velocity zone at the base of the mantle beneath the central Pacific. *Phys. Earth Planet. Inter.* **184,** 119–133 (2011).
66. Garnero, E. Heterogeneity of the lowermost mantle. *Annu. Rev. Earth Planet. Sci.* **28,** 509–537 (2000).
67. Ishii, M. & Tromp, J. Normal-mode and free-air gravity constraints on lateral variations in velocity and density of Earth's mantle. *Science* **285,** 1231–1236 (1999).
68. Tarduno, J. *et al.* The Emperor Seamounts: Southward motion of the Hawaiian hotspot plume in Earth's mantle. *Science* **301,** 1064–1069 (2003).
69. Wolfe, C. J. *et al.* Mantle P-wave velocity structure beneath the Hawaiian hotspot. *Earth Planet. Sci. Lett.* **303,** 267–280 (2011).
70. Richards, M. A. & Griffiths, R. W. Thermal entrainment by deflected mantle plumes. *Nature* **342,** 900–902 (1989).
71. Kerr, R. C. & Lister, J. R. Rise and deflection of mantle plume tails. *Geochem. Geophys. Geosyst.* **9**, Q10004 (2008).
72. Blichert-Toft, J. & Albarède, F. Mixing of isotopic heterogeneities in the Mauna Kea plume conduit. *Earth Planet. Sci. Lett.* **282,** 190–200 (2009).
73. Blake, S. & Campbell, I. The dynamics of magma-mixing during flow in volcanic conduits. *Contrib. Mineral. Petrol.* **94,** 72–81 (1986).
74. Lister, J. Long-wavelength instability of a line plume. *J. Fluid Mechanics* **175,** 413–428 (1987).
75. Cao, Q., der Hilst, van, R., de Hoop, M. & Shim, S. Seismic imaging of transition zone discontinuities suggests hot mantle west of Hawaii. *Science* **332,** 1068–1071 (2011).
76. Olson, P. & Yuen, D. A. Thermochemical plumes and mantle phase transitions. *J. Geophys. Res.* **87,** 3993–4002 (1982).
77. Hirose, K. Phase transitions in pyrolitic mantle around 670-km depth: Implications for upwelling of plumes from the lower mantle. *J. Geophys. Res.* **107**, B42078 (2002).
78. Boschi, L., Becker, T. & Steinberger, B. Mantle plumes: Dynamic models and seismic images. *Geochem. Geophys. Geosyst.* **8**, Q10006 (2007).
79. Bercovici, D. & Mahoney, J. Double flood basalts and plume head separation at the 660 kilometer discontinuity. *Science* **266,** 1367–1369 (1994).
80. Kumagai, I. & Kurita, K. On the fate of mantle plumes at density interfaces. *Earth Planet. Sci. Lett.* **179,** 63–71 (2000).
81. Lister, J. & Kerr, R. C. The propagation of two-dimensional and axisymmetric viscous gravity currents at a fluid interface. *J. Fluid Mechanics* **203,** 215–249 (1989).
82. Steinberger, B., Sutherland, R. & O'Connell, R. J. Prediction of Emperor–Hawaii seamount locations from a revised model of global plate motion and mantle flow. *Nature* **430,** 167–173 (2004).
83. Garnero, E., Lay, T. & McNamara, A. in *Plates, Plumes, and Planetary Processes* (eds Foulger, G. R. & Jurdy, D. M.), *Geol. Soc. Am. Spec. Paper* **430**, 79–101 (2007).
84. Idehara, K. Structural heterogeneity of an ultra-low-velocity zone beneath the Philippine Islands: Implications for core–mantle chemical interactions induced by massive partial melting at the bottom of the mantle. *Phys. Earth Planet. Inter.* **184,** 80–90 (2011).
85. McNamara, A., Garnero, E. & Rost, S. Tracking deep mantle reservoirs with ultra-low velocity zones. *Earth Planet. Sci. Lett.* **299,** 1–9 (2010).
86. Williams, Q., Revenaugh, J. & Garnero, E. A correlation between ultra-low basal velocities in the mantle and hot spots. *Science* **281,** 546–549 (1998).
87. Rost, S., Garnero, E., Williams, Q. & Manga, M. Seismological constraints on a possible plume root at the core–mantle boundary. *Nature* **435,** 666–669 (2005).
88. Nomura R. *et al.* Spin crossover and iron-rich silicate melt in the Earth's deep mantle. *Nature* **473,** 199–202 (2011).
89. Hernlund, J. W. & Jellinek, A. M. Dynamics and structure of a stirred partially molten ultralow-velocity zone. *Earth Planet. Sci. Lett.* **296,** 1–8 (2010).
90. Maclennan, J. Lead isotope variability in olivine-hosted melt inclusions from Iceland. *Geochim. Cosmochim. Acta* **72,** 4159–4176 (2008).
91. Hewitt, I. J. Modelling melting rates in upwelling mantle. *Earth Planet. Sci. Lett.* **300,** 264–274 (2010).
92. Williams, Q. & Garnero, E. J. Seismic evidence for partial melt at the base of the mantle, *Science* **273,** 1528–1530 (1996).
93. Brandon, A. D. & Walker, R. J. The debate over core–mantle interaction. *Earth Planet. Sci. Lett.* **232,** 211–225 (2005).
94. Murphy, D. T., Brandon, A. D., Debaille, V., Burgess, R. & Ballentine, C. J. In search of a hidden long-term isolated sub-chondritic $^{142}Nd/^{144}Nd$ reservoir in the deep mantle: Implications for the Nd isotope systematics of the Earth. *Geochim. Cosmochim. Acta* **74,** 738–750 (2010).
95. Vidal, V. & Bonneville, A. Variations of the Hawaiian hot spot activity revealed by variations in the magma production rate. *J. Geophys. Res.* **109**, B03104 (2004).
96. Huang, S., Hall, P. S. & Jackson, M. G. Geochemical zoning of volcanic chains associated with Pacific hotspots. *Nature Geosci.* http://dx.doi.org/10.1038/ngeo1263 (2011).
97. Weis, D., Bassias, Y., Gautier, I. & Mennessier, J. Dupal anomaly in existence 115 Ma ago — evidence from isotopic study of the Kerguelen Plateau (South Indian Ocean). *Geochim. Cosmochim. Acta* **53,** 2125–2131 (1989).
98. Ni, S., Tan, E., Gurnis, M. & Helmberger, D. V. Sharp sides to the African super plume. *Science* **296,** 1850–1852 (2002).
99. Hart S. R. A large-scale isotope anomaly in the Southern Hemisphere mantle, *Nature* **309,** 753–757 (1984).
100. Wen, L. A compositional anomaly at the Earth's core-mantle boundary as an anchor to the relatively slowly moving surface hotspots and as source to the DUPAL anomaly. *Earth Planet. Sci. Lett.* **246,** 138–148 (2006).
101. Regelous, M., Hofmann, A. W., Abouchami, W. & Galer, S. J. G. Geochemistry of lavas from the Emperor Seamounts, and the geochemical evolution of Hawaiian magmatism from 85 to 42 Ma. *J. Petrol.* **44,** 113–140 (2003).
102. US Geological Survey. Bathymetric map of the Hawaiian Islands (2003), available at http://geopubs.wr.usgs.gov/i-map/i2809.
103. Geochemistry of Rocks of the Oceans and Continents (GEOROC) database, available at http://georoc.mpch-mainz.gwdg.de/georoc/.
104. Trusdell, F. A. & Lockwood, J. P. Geologic Maps of the Northeast Flank of, Central-Southeast Flank of, Southern Mauna Loa Volcano, Island of Hawai'i, Hawai'i: US Geological Survey SIM 2932-A, SIM 2932-B, SIM 2932-C respectively, scale 1:50,000 (in the press).
105. Grand, S. P. Mantle shear-wave tomography and the fate of subducted slabs. *Phil. Trans. R. Soc. A* **360,** 2475–2491 (2002).
106. Steinberger, B. Plumes in a convecting mantle: Models and observations for individual hotspots. *J. Geophys. Res.* **105,** 11127–11152 (2000).
107. Bréger, L. & Romanowicz, B. Three-dimensional structure at the base of the mantle beneath the central Pacific. *Science* **282,** 718–720 (1998).

Acknowledgements

We thank D. DePaolo, A. Hofmann, D. Hanano, A. Greene, I. Nobre Silva, C. Farnetani, F. Albarède and numerous PCIGR graduate students for discussions and insights into mantle geochemistry. We thank C. Maerschalk (ULB), B. Kieffer and J. Barling (PCIGR, UBC) for helping to produce the data. We thank S. Sparks, VGP President, for inviting D.W. to give the Daly Lecture at Fall AGU 2010. Financial support was provided by the Belgian Fonds National de la Recherche Scientifique (FNRS), NSERC Discovery Grants to D.W., J.S.S. and A.M.J., and NSF grants to M.O.G. and J.M.R. A.M.J. also acknowledges support from the Canadian Institute for Advanced Research. Correspondence and requests for materials should be addressed to D.W.

Author contributions

D.W. acquired the data, compiled the literature data, conceived the idea for the paper and developed the conceptual model with A.M.J. D.W. wrote the paper, together with A.M.J and J.S.S. All authors discussed the results and the model, and contributed to the manuscript. M.O.G. and J.M.R. also wrote the proposals, led the expeditions and organized the sampling on Hawai'i and shared their knowledge and data on these islands.

Additional Information

The authors declare no competing financial interests.
Supplementary Information accompanies this paper on www.nature.com/naturegeoscience.

© 2011 Macmillan Publishers Limited. All rights reserved

nature geoscience

SUPPLEMENTARY INFORMATION

DOI: 10.1038/NGEO1328

Role of the deep mantle in generating the compositional asymmetry of the Hawaiian mantle plume

Weis et al.

Supplementary Information: table of contents.

© 2011 Macmillan Publishers Limited. All rights reserved.

Role of the deep mantle in generating the compositional asymmetry of the Hawaiian mantle plume
Weis et al.

Supplementary Information

Table S1 | Complete data table for new Mauna Loa isotopic analyses (~120 shield lava samples)

Submarine southwest rift zone															
Samples	Depth (mbsl)	$^{87}Sr/^{86}Sr$	2σ	$^{143}Nd/^{144}Nd$	2σ	ε_{Nd}	$^{206}Pb/^{204}Pb$	2σ	$^{207}Pb/^{204}Pb$	2σ	$^{208}Pb/^{204}Pb$	2σ	$^{176}Hf/^{177}Hf$	2σ	ε_{Hf}
Jason 2 Mile High basalts															
J2-016-01	2290	0.703768	7	0.512943	6	5.9	18.1602	16	15.4671	18	37.9244	45	0.283081	8	10.9
J2-019-01	2016	0.703703	7	0.512933	6	5.7	18.2615	16	15.4627	13	38.0147	35	0.283077	8	10.8
J2-019-04	1986	0.703746	7	0.512914	6	5.4	18.1816	23	15.4605	20	37.9780	50	0.283052	10	9.9
J2-019-08	1805	0.703697	7	0.512913	5	5.4	18.2163	24	15.4774	23	38.0610	62	0.283052	14	9.9
J2-019-10	1753	0.703677	6	0.512936	5	5.8	18.1831	20	15.4620	16	37.9472	45	0.283073	11	10.6
J2-019-19	1401	0.703748	8	0.512907	5	5.2	18.1532	18	15.4560	20	37.9824	51	0.283061	11	10.2
J2-019-22	1350	0.703680	9	0.512943	5	5.9	18.1738	22	15.4581	21	37.9317	60	0.283077	9	10.8
J2-020-01	1353	0.703818	7	0.512882	6	4.8	18.1248	34	15.4545	26	38.0208	64	0.283004	18	8.2
J2-020-01*		0.703811	8	0.512875	7	4.6	18.1232	19	15.4498	16	38.0157	43	0.282916	4	5.1
J2-020-03	1296	0.703674	8	0.512943	8	5.9	18.1784	15	15.4588	13	37.9384	34	0.283078	7	10.8
J2-020-03*		0.703682	6	0.512946	6	6.0	18.1769	12	15.4578	10	37.9345	29	0.283092	6	11.3
J2-020-09	1093	0.703668	8	0.512947	6	6.0	18.1803	12	15.4570	8	37.9367	29	0.283091	8	11.3
J2-020-14	857	0.703681	9	0.512963	5	6.3	18.1557	14	15.4594	12	37.8982	34	0.283104	8	11.7
J2-020-20	600	0.703691	8	0.512936	6	5.8	18.1807	8	15.4580	8	37.9406	23	0.283086	5	11.1
J2-020-23	489	0.703681	5	0.512940	5	5.9	18.1789	14	15.4547	13	37.9341	33	0.283092	6	11.3
Standard analyses		NBS 987	n=19	La Jolla	n=34								JMC 475	n=10	
		0.710262	10	0.511853	9								0.282159	14	
Pisces Dives															
184-2	1735	0.703725	3	0.512943	8	6.0	18.1851	24	15.4477	21	37.9945	53	0.283086	5	11.1
184-7	1240	0.703820	5	0.512894	92	5.0	18.1316	21	15.4578	17	38.0340	48	0.283066	5	10.4
184-8	1020	0.703668	7	0.512944	10	6.0	18.1684	16	15.4490	15	37.9068	41	0.283088	5	11.2
184-9	775	0.703677	3	0.512956	8	6.2	18.1544	21	15.4569	19	37.8935	47	0.283101	5	11.7
184-10	755	0.703680	4	0.512933	8	5.8	18.1905	19	15.4468	16	37.9240	45	0.283085	5	11.1
184-11	745	0.703654	8	0.512958	16	6.2	18.1828	29	15.4520	24	37.9133	50	0.283103	6	11.7
184-12	575	0.703694	6	0.512952	12	6.1	18.1493	24	15.4463	22	37.8805	60	0.283084	5	11.0
184-12 #2													0.283095	6	11.4
184-13	550	0.703686	4	0.512951	8	6.1	18.1505	25	15.4478	23	37.8866	53	0.283091	5	11.3
185-5	1670	0.703772	4	0.512915	10	5.4	18.2488	31	15.4553	26	38.0538	67	0.283072	5	10.6
185-10	1515	0.703683	8	0.512942	14	5.9	18.1770	26	15.4615	25	37.9328	66	0.283086	5	11.1
Dredging															
M4-14-1	4500	0.703668	4	0.512939	8	5.9	18.1665	20	15.4518	17	37.9162	47	0.283094	5	11.4
M18-17-1	3100	0.703679	6	0.512962	6	6.3	18.1846	19	15.4501	17	37.9086	45	0.283097	7	11.5
M18-17-1 #2													0.283100	6	11.6
M19-2-1	2400	0.703840	7	0.512860	18	4.3	18.1087	24	15.4429	21	38.0093	53	0.283069	5	10.5
M19-17-1	2400	0.703812	5	0.512880	20	4.7	18.1257	11	15.4461	10	37.9959	29	0.283067	6	10.4
Other Submarine Dredged															
Radial Vents															
M22-4-3	2100	0.703669	6	0.512939	12	5.9	18.1769	30	15.4497	28	37.9090	63	0.283084	5	11.0
M24-8-3	2100	0.703909	0	0.512868	5	4.5	18.0568	12	15.4521	12	37.8682	33			
M27-11-3	2100	0.703772	5	0.512940	10	5.9	18.1362	14	15.4606	13	37.8744	34	0.283087	8	11.1
J2-026-2	1925	0.703679	8	0.512950	5	6.1	18.1617	15	15.4521	15	37.9212	38			
J2-026-10	1472	0.703884	8	0.512890	5	4.9	18.0937	11	15.4612	11	37.8655	29			
Slope															
M8-1-2	3500	0.703688	4	0.512953	6	6.1	18.1663	18	15.4496	15	37.9029	49	0.283089	5	11.2
M17-2-2	1700	0.703661	5	0.512944	9	6.0	18.1582	13	15.4529	12	37.9039	34	0.283088	4	11.2
M26-14-2	2900	0.703765	6	0.512924	11	5.6	18.1075	18	15.4518	18	37.8441	33	0.283077	7	10.8
M30-1-2	3700	0.703739	5	0.512923	12	5.6	18.1509	25	15.4508	23	37.9017	55	0.283076	9	10.7
Landslides															
M12-3-4	3700	0.703607	4	0.512944	10	6.0	18.3494	17	15.4634	14	38.0687	37	0.283084	4	11.0
M13-2-4	4400	0.703667	4	0.512975	10	6.6	18.2091	10	15.4570	9	37.8898	25	0.283117	5	12.2
M13-12-4	4400	0.703659	4	0.512916	4	5.4	18.3414	19	15.4696	16	38.1189	42	0.283082	6	11.0
M13-21-4	4400	0.703667	5	0.512965	12	6.4	18.3951	17	15.4712	14	38.1619	30	0.283087	8	11.1
M14-20-4	4400	0.703738	4	0.512920	16	5.5	18.1992	13	15.4509	13	37.9871	33	0.283072	6	10.6
M14-32-4	4400	0.703691	3	0.512946	10	6.0	18.1663	72	15.4530	61	37.9289	151	0.283083	8	11.0
Standard analyses		NBS 987	n=19	Rennes	n=8								JMC 475	n=28	
		0.710249	10	0.511970	5								0.282162	7	

© 2011 **Macmillan Publishers Limited. All rights reserved.**

Supplementary Information
Table S1 | Complete data table for new Mauna Loa isotopic analyses (~120 shield lava samples), continued

Subaerial															
Samples	Depth (mbsl)	$^{87}Sr/^{86}Sr$	2σ	$^{143}Nd/^{144}Nd$	2σ	ε_{Nd}	$^{206}Pb/^{204}Pb$	2σ	$^{207}Pb/^{204}Pb$	2σ	$^{208}Pb/^{204}Pb$	2σ	$^{176}Hf/^{177}Hf$	2σ	ε_{Hf}
HSDP-1	Depth in m														
R-126	199.8	0.703698	9	0.512941	6	5.9	18.2333	30	15.4665	26	37.9734	63	0.283092	6	11.3
R-121	191.8	0.703694	7	0.512939	6	5.9	18.2288	17	15.4590	19	37.9575	46	0.283085	5	11.1
R-114	176.1	0.703734	7	0.512946	6	6.0	18.0494	24	15.4405	21	37.7896	63	0.283097	5	11.5
R-110	164	0.703709	7	0.512938	8	5.9	18.1735	22	15.4639	20	37.9152	59	0.283084	5	11.0
R-91	129.2	0.703679	6	0.512946	6	6.0	18.2495	45	15.4570	36	37.9438	94	0.283092	6	11.3
R-68	94.1	0.703805	7	0.512919	7	5.5	18.1043	31	15.4604	26	37.8411	63	0.283080	6	10.9
Standard analyses		NBS 987	n=19	La Jolla	n=7								JMC 475	n=12	
		0.710262	10	0.511857	9								0.282170	11	
Prehistoric	Age in ka"														
L00 525	36.8	0.703700	9	0.512934	7	5.8	18.2119	24	15.4528	22	37.9706	62	0.283075	5	10.7
L91 564	29.0	0.703932	7	0.512914	6	5.4	18.0964	14	15.4609	10	37.8457	40	0.283074	8	10.7
L00 003	28.1	0.703753	6	0.512951	6	6.1	18.0939	25	15.4522	23	37.8145	70	0.283095	5	11.4
L00 503	26.6	0.703746	9	0.512949	6	6.1	18.1425	27	15.4528	23	37.8640	56	0.283083	5	11.0
L00 506	26.0	0.703714	7	0.512951	6	6.1	18.1946	21	15.4635	19	37.9353	55	0.283095	6	11.4
L91 55	10.0	0.703764	6	0.512954	7	6.2	18.0826	19	15.4473	17	37.8322	47	0.283081	11	10.9
L87 235	9.3	0.703732	7	0.512937	6	5.8	18.0910	39	15.4558	34	37.8614	109	0.283080	9	10.9
L93 753	5.9	0.703930	7	0.512885	6	4.8	18.0818	29	15.4588	26	37.8511	63	0.283054	6	10.0
L00 002	4.1	0.703876	6	0.512897	6	5.1	18.0560	22	15.4526	19	37.8227	52	0.283050	6	9.8
L93 733	3.7	0.703907	7	0.512871	8	4.6	18.1068	17	15.4602	16	37.8901	45	0.283046	6	9.7
L00 014	3.1	0.703757	7	0.512952	7	6.1	18.2227	29	15.4592	24	37.9361	58	0.283088	5	11.2
Standard analyses		NBS 987	n=11	La Jolla	n=5								JMC 475	n-12	
		0.710269	11	0.511853	7								0.282170	11	
Historical	Year														
ML-20	1843	0.703948	7	0.512867	6	4.5	18.0753	12	15.4650	12	37.8837	34			
ML-20 #2							18.0723	11	15.4636	10	37.8821	26			
ML-20 #3							18.0739	15	15.4633	13	37.8830	35			
ML-52	1852	0.703903	6	0.512866	6	4.5	18.0856	9	15.4656	9	37.8847	22			
ML-46	1855	0.703832	8	0.512918	8	5.5	18.0964	8	15.4645	7	37.8659	20			
ML-71	1859	0.703805	8	0.512914	5	5.4	18.1315	33	15.4627	26	37.8857	68			
ML-71 #2							18.1356	15	15.4663	12	37.8965	35			
ML-83	1868	0.703861	8	0.512899	6	5.1	18.1153	15	15.4587	14	37.8797	38			
J2-14-12^	1877	0.703839	7	0.512896	8	5.0	18.1502	23	15.4607	18	37.8955	45			
J2-18-12^	1877	0.703851	7	0.512907	6	5.2	18.1502	16	15.4621	13	37.8999	36			
ML-41	1880	0.703848	8	0.512923	6	5.6	18.1720	13	15.4629	13	37.9115	35			
ML-41 #2							18.1764	15	15.4684	12	37.9258	32			
ML-41 #3							18.1723	20	15.4631	22	37.9135	64			
ML-45	1880	0.703820	6	0.512908	6	5.3	18.1515	11	15.4653	9	37.9100	26			
ML-95	1887	0.703815	7	0.512929	7	5.7	18.1682	11	15.4643	9	37.9203	26			
ML-91	1907	0.703763	10	0.512933	6	5.8	18.1611	14	15.4647	13	37.9071	38			
ML-63	1919	0.703791	7	0.512936	8	5.8	18.1330	5	15.4639	5	37.8826	14			
ML-90	1926	0.703803	8	0.512921	7	5.5	18.1154	8	15.4616	7	37.8733	18			
ML-34	1935	0.703804	8	0.512923	6	5.6	18.1060	8	15.4598	7	37.8663	19			
ML-129	1940	0.703832	7	0.512919	6	5.5	17.8158	7	15.4936	7	37.5821	19			
ML-129 #2							17.8176	6	15.4951	6	37.5876	14			
ML-37	1942	0.703804	6	0.512911	6	5.3	18.1005	6	15.4591	6	37.8638	16			
ML-81	1949	0.703814	8	0.512919	6	5.5	18.0947	8	15.4596	7	37.8682	19			
ML-281	1950	0.703840	7	0.512906	7	5.2	18.0843	19	15.4593	17	37.8659	43			
ML-126	1975	0.703853	7	0.512908	6	5.3	18.0841	8	15.4580	8	37.8595	21			
ML-190	1984	0.703854	7	0.512895	11	5.0	18.0816	14	15.4584	13	37.8629	35			
ML-190*	1984	0.703854	7	0.512899	6	5.1	18.0833	16	15.4600	14	37.8680	35			
Standard analyses		NBS 987	n=3, 7	La Jolla	n=3, 11										
	Series 1	0.710257	24	0.511847	14										
	Series 2	0.710253	13	0.511853	11										

* Complete duplicate analysis, including leaching.
The 2σ error is the absolute error value of the individual sample analysis (internal error), reported to the significant digit.
^ Radial vent, data from Wanless et al., 2006.
" C-14 ages in ka, as reported in the Mauna Loa maps (Trusdell & Lockwood, in press).
2 or 3 Replicate analysis for the Pb or Hf isotopic compositions on the Nu Plasma MC-ICP-MS.

© 2011 **Macmillan Publishers Limited. All rights reserved.**

References for Data sources

Hilina: Kimura, J., Sisson, T., Nakano, N., Coombs, M. & Lipman, P. Isotope geochemistry of early Kilauea magmas from the submarine Hilina bench: The nature of the Hilina mantle component. *J. Volc. Geotherm. Res.* **151**, 51–72 (2006).

Hana Ridge: Ren, Z.-Y., Tomoyuki, S., Masako, Y., Johnson, K. M. & Takahashi, E. Isotope compositions of submarine Hana Ridge lavas, Haleakala volcano, Hawaii: Implications for source compositions melting process and the structure of the Hawaiian plume. *J. Petrol.* **47**, 255–275 (2006).

Kīlauea historic, prehistoric: Abouchami, W. *et al*. Lead isotopes reveal bilateral asymmetry and vertical continuity in the Hawaiian mantle plume. *Nature* **434**, 851–856 (2005). Marske, J.P., Pietruszka, A.J., Weis, D., Garcia, M.O. & Rhodes, J.M. Rapid passage of a small-scale mantle heterogeneity through the melting regions of Kilauea and Mauna Loa Volcanoes. *Earth Planet. Sci. Lett.* **259**, 34–50 (2007).

Mauna Kea Hi-8, Mid-8 and Lo-8: Eisele, J., Abouchami, W., Galer, S.J.G. & Hofmann, A.W. The 320 kyr Pb isotope evolution of Mauna Kea lavas recorded in the HSDP-2 drill core. *Geochem. Geophys. Geosyst*. **4**, 8710 (2003).

Kohala: Abouchami, W. *et al*. Lead isotopes reveal bilateral asymmetry and vertical continuity in the Hawaiian mantle plume. *Nature* **434**, 851–856 (2005).

West Maui: Gaffney, A., Nelson, B. & Blichert-Toft, J. Geochemical constraints on the role of oceanic lithosphere in intra-volcano heterogeneity at West Maui, Hawaii. *J. Petrol.* **45**, 1663–1687 (2004).

East Moloka‘i: Xu, G., Frey, F.A., Clague, D.A., Weis, D. & Beeson, M. East Molokai and other Kea-trend volcanoes: Magmatic processes and sources as they migrate away from the Hawaiian hot spot. *Geochem. Geophys. Geosyst.* **6**, Q05008 (2005).

© 2011 **Macmillan Publishers Limited. All rights reserved.**

West Moloka‘i: Xu, G. *et al.* Geochemical characteristics of West Molokai shield- and postshield-stage lavas: Constraints on Hawaiian plume models. *Geochem. Geophys. Geosyst.* **8**, Q08G21 (2007).

Lō‘ihi: Abouchami, W. *et al*. Lead isotopes reveal bilateral asymmetry and vertical continuity in the Hawaiian mantle plume. *Nature* **434**, 851–856 (2005).
Mauna Loa HSDP-II: Blichert-Toft, J., Weis, D., Maerschalk, C., Agranier, A. & Albarède, F. Hawaiian hot spot dynamics as inferred from the Hf and Pb isotope evolution of Mauna Kea volcano. *Geochem. Geophys. Geosyst.* **4**, 8704 (2003).
Mauna Loa early prehistoric: Marske, J.P., Pietruszka, A.J., Weis, D., Garcia, M.O. & Rhodes, J.M. Rapid passage of a small-scale mantle heterogeneity through the melting regions of Kilauea and Mauna Loa Volcanoes. *Earth Planet. Sci. Lett.* **259**, 34–50 (2007).
Mauna Loa SW rift zone, this paper
Mauna Loa HSDP-1: Abouchami, W. *et al*. Lead isotopes reveal bilateral asymmetry and vertical continuity in the Hawaiian mantle plume. *Nature* **434**, 851–856 (2005).
Mauna Loa HSDP-1, this paper
Mauna Loa Historic >1850, this paper
Mauna Loa Mile High Section, this paper
Mauna Loa radial vents: Wanless, V.D*. et al.* Submarine radial vents on Mauna Loa Volcano, Hawai`i. *Geochem. Geophys. Geosyst.* **7**, Q05001 (2006).
Hualalai North Kona: Yamasaki, S., Kani, T., Hanan, B. & Tagami, T. Isotopic geochemistry of Hualalai shield-stage tholeiitic basalts from submarine North Kona region, Hawaii. *J. Volc. Geoth. Res.* **185**, 223–230 (2009).
Mahukona: Hanano, D., Weis, D., Scoates, J.S., Aciego, S. & DePaolo, D.J. Horizontal and vertical zoning of heterogeneities in the Hawaiian mantle plume from the geochemistry of consecutive postshield volcano pairs: Kohala-

© 2011 **Macmillan Publishers Limited. All rights reserved.**

Mahukona and Mauna Kea-Hualalai. *Geochem. Geophys. Geosyst.* **11**, Q01004 (2010).
Kaho‘olawe: Abouchami, W. *et al*. Lead isotopes reveal bilateral asymmetry and vertical continuity in the Hawaiian mantle plume. *Nature* **434**, 851–856 (2005).
Kaho‘olawe: Huang, S. *et al*. Enriched components in the Hawaiian plume: Evidence from Kahoolawe Volcano, Hawaii. *Geochem. Geophys. Geosyst.* **6**, Q11006 (2005).
Lāna‘i: Abouchami, W. *et al*. Lead isotopes reveal bilateral asymmetry and vertical continuity in the Hawaiian mantle plume. *Nature* **434**, 851–856 (2005).
Lāna‘i: Gaffney, A., Nelson, B. & Blichert-Toft, J. Melting in the Hawaiian plume at 1-2 Ma as recorded at Maui Nui: The role of eclogite, peridotite, and source mixing. *Geochem. Geophys. Geosyst.* **6**, Q10L11 (2005).
Ko‘olau KSDP: Fekiacova, Z., Abouchami, W., Galer, S.J.G., Garcia, M.O. & Hofmann, A.W. Origin and temporal evolution of Ko'olau Volcano, Hawai‘i: Inferences from isotope data on the Ko’olau Scientific Drilling Project (KSDP), the Honolulu Volcanics and ODP Site 843. *Earth Planet. Sci. Lett.* **261**, 65-83 (2007).
Ko‘olau Nu‘uanu and Makapu‘u: Tanaka, R., Makishima, A. & Nakamura, E. Hawaiian double volcanic chain triggered by an episodic involvement of recycled material: Constraints from temporal Sr-Nd-Hf-Pb isotopic trend of the Loa-type volcanoes. *Earth Planet. Sci. Lett.* **265**, 450–465 (2008). Tanaka, R., Nakamura, E. & Takahashi, E. Geochemical evolution of Koolau volcano, Hawaii, in: *Hawaiian Volcanoes: Deep Underwater Perspectives* (eds. Takahashi, E., Lipman, P.W., Garcia, M.O., Naka, J., Aramaki, S.). G*eophys. Monogr. Ser.* **128**, American Geophysical Union, Washington, DC, 311–332 (2002).
Ko‘olau: Abouchami, W. *et al*. Lead isotopes reveal bilateral asymmetry and vertical continuity in the Hawaiian mantle plume. *Nature* **434**, 851–856 (2005).
West Ka‘ena: Greene, A.R. *et al.* Low-productivity Hawaiian volcanism between Kaua‘i and O‘ahu. *Geochem. Geophys. Geosyst.* **11**, Q0AC08 (2010).

© 2011 **Macmillan Publishers Limited. All rights reserved.**

Kaua‘i: Garcia, M.O. *et al.* Petrology, geochemistry and geochronology of Kaua'i lavas over 4.5 Myr: implications for the origin of rejuvenated volcanism and the evolution of the Hawaiian plume. *J. Petrol.* **51**, 1507–1540 (2010).
Wai‘anae: Coombs, M., Clague, D.A., Moore, J.G. & Cousens, B.L. Growth and collapse of Waianae Volcano, Hawaii, as revealed by exploration of its submarine flanks. *Geochem. Geophys. Geosyst.* **5**, Q08006 (2004).

Figure 2 | Isotopic data for Hawaiian shield lavas, extended caption. **a,** $^{208}Pb/^{204}Pb$ vs. $^{206}Pb/^{204}Pb$ for all Hawaiian shield lavas (>700 samples, all high-precision data and all normalized to the same standard values, Supplementary information: Analytical techniques). Kea trend volcanoes are represented by circles and warm (red, orange, yellow, brown) colors, whereas Loa trend volcanoes are represented by diamonds and cool (blue, green, mauve) colors. Triple-spike literature data are indicated by a darker outline. Both Mauna Loa and Mauna Kea samples have larger symbols. Mauna Loa trend and Mauna Kea trend volcanoes have different Pb isotopic compositions and the boundary separating their data points is highlighted by the thick black line[27]. Insets: The two small insets show the Pb-Pb arrays among some of the individual volcanoes. Solid lines are for the two volcanoes from the Big Island (Mauna Loa: HSDP-I and Mile High Section; Mauna Kea: low-, mid- and high-8), whereas dashed lines are for samples from the other Hawaiian volcanoes/features (Loa trend: Li: Lō‘ihi, H: Hualālai, L: Lāna‘i, K: Kaho‘olawe; Kea trend: Ha: Hana Ridge, Ki: Kīlauea, Ko: Kohala, M: Maui, EM: East Moloka‘i, WM: West Moloka‘i). **b,** $^{208}Pb^*/^{206}Pb^*$ vs. ε_{Nd} for Hawaiian shield lavas. $^{208}Pb^*/^{206}Pb^*$ is a measure of the radiogenic addition to $^{208}Pb/^{204}Pb$ and $^{206}Pb/^{204}Pb$ during Earth history and is calculated by subtracting the primordial (initial) isotope ratios from the measured values. $^{208}Pb^*/^{206}Pb^*$ reflects the ratio of Th/U integrated over the history of the Earth. ε_{Nd} is a measure of the deviation of the $^{143}Nd/^{144}Nd$ ratio from the chondritic value ($^{143}Nd/^{144}Nd = 0.512638$), assumed to be identical to the present-day value in the

© 2011 Macmillan Publishers Limited. All rights reserved.

bulk silicate earth. Inset: $^{208}Pb^*/^{206}Pb^*$ vs. ε_{Nd} detail of Mauna Loa lavas (this study, plus Prehistoric lavas <3ka[45], Radial vents[52]) – older Mauna Loa samples (red, yellow and orange diamonds, Supplementary Fig. S1) sampled along the submarine southwest rift zone define a mixing trend (steeper slope in this plot) not observed anywhere else on the islands. All data sources are reported, listed by volcano along the Kea and Loa chains, in the supplementary online material.

© 2011 **Macmillan Publishers Limited. All rights reserved.**

Supplementary figure

Figure S1 | Isotopic plots of Mauna Loa lavas (this study and literature data: Radial vents[1], HSDP-II[2], Prehistoric <3ka[3]). **a,** $^{143}Nd/^{144}Nd$ vs. $^{87}Sr/^{86}Sr$. **b,** $^{208}Pb/^{206}Pb$ vs. $^{207}Pb/^{206}Pb$. **c,** $^{208}Pb/^{204}Pb$ vs. $^{206}Pb/^{204}Pb$.

1. Wanless, V.D. et al. Submarine radial vents on Mauna Loa Volcano, Hawai`i. *Geochem. Geophys. Geosyst.* **7**, Q05001 (2006).
2. Blichert-Toft, J., Weis, D., Maerschalk, C., Agranier, A. & Albarède, F. Hawaiian hot spot dynamics as inferred from the Hf and Pb isotope evolution of Mauna Kea volcano. *Geochem. Geophys. Geosyst.* **4**, 8704 (2003).
3. Marske, J.P., Pietruszka, A.J., Weis, D., Garcia, M.O. & Rhodes, J.M. Rapid passage of a small-scale mantle heterogeneity through the melting regions of Kilauea and Mauna Loa Volcanoes. *Earth Planet. Sci. Lett.* **259**, 34–50 (2007).

© 2011 **Macmillan Publishers Limited. All rights reserved.**

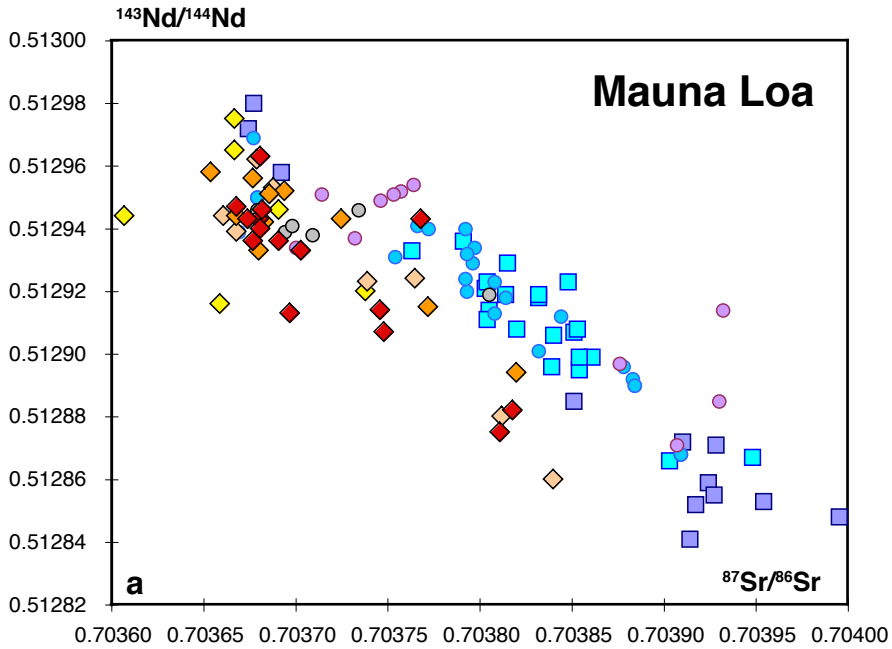

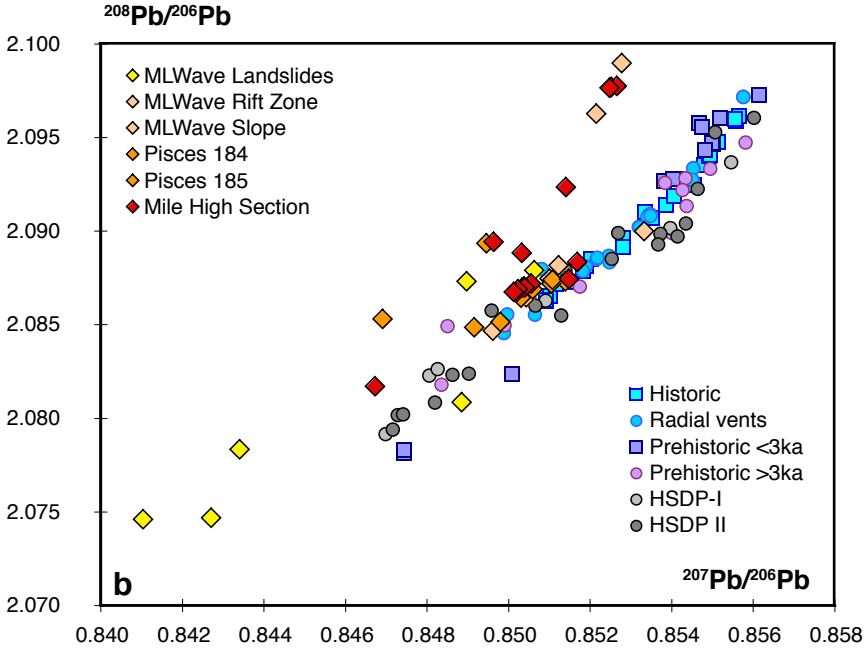

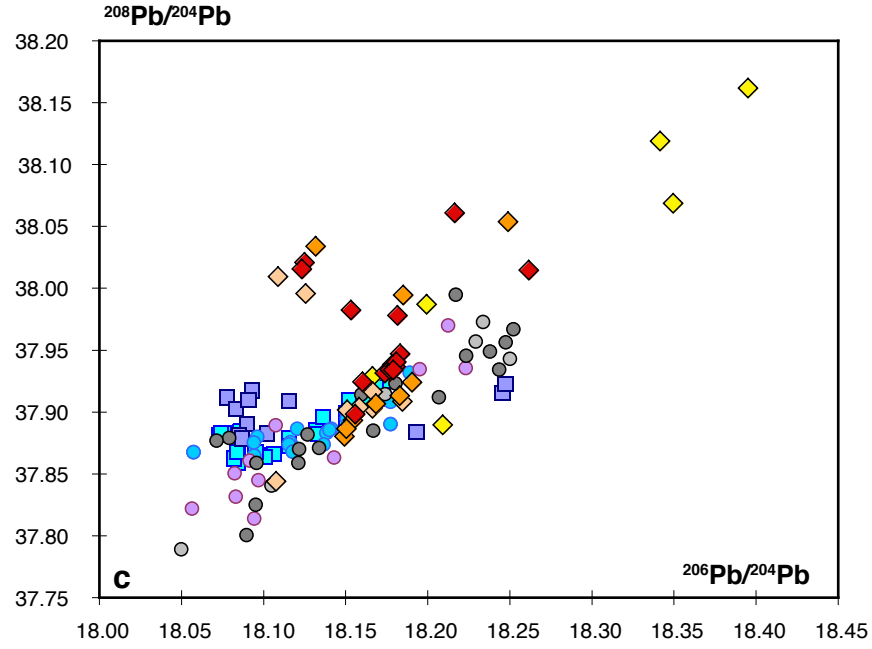

Weis et al. Supplementary Figure S1

© 2011 Macmillan Publishers Limited. All rights reserved.

Supplementary Information: Analytical techniques

Brief description of sample preparation, reference materials and standards, normalization of literature data.

Whole-rock powders of these Mauna Loa samples were analyzed for Pb, Sr, Nd and Hf isotope ratios using methods described in 1,2. All isotope ratios were measured at the Pacific Centre for Isotopic and Geochemical Research (PCIGR) at the University of British Columbia (UBC) with a Finnigan Triton thermal ionization mass spectrometer (TIMS) for Sr and Nd and with a Nu Plasma multiple-collector inductively coupled plasma mass spectrometer (MC-ICP-MS) for Pb and Hf. All the samples were previously leached following the procedure described in 3 to eliminate secondary alteration and potential contamination during sample handling (especially for the drilled samples[4]) as observed in the HSDP-I samples[5]). The number of leaching steps varied between 6 and 8 times 20 min in 6N HCl in an ultrasonic bath, followed by two rinses of 18 megaohm water. The leaching process was stopped when a visually clear solution (i.e., colorless and without suspension) was obtained. The corresponding weight loss varied between 12 and 48%. Careful leaching is critical for achieving high-precision and reproducibility in Pb (<200 ppm) and Sr (<30 ppm) isotopes that is otherwise not possible[6].

The chemical separation and mass spectrometry procedures are described in detail in 1,2 and included a double pass on columns for Pb isotopic analyses to reduce matrix effects and improve accuracy[4,7]. The reproducibility of the isotopic analyses at PCIGR was based on repeated analyses of USGS reference materials, as well as duplicate and replicate analyses of some of the samples (see Table S1). In addition, the accuracy of the analysis was controlled by repeated analyses of standard materials: SRM 987 Sr standard, La Jolla and Rennes Nd standard, JMC 475 (original solution distributed by Jon Patchett, University of Arizona) and SRM 981 Pb standard.

© 2011 **Macmillan Publishers Limited. All rights reserved.**

Isotopic results for the Mile High Section, the Pisces and dredge samples along the submarine southwest rift zone, historical lavas, and HSDP-I Mauna Loa lavas are reported in Table S1. The 2σ error is the measured absolute error value of the individual sample analysis (internal error). For comparison purposes, all literature data (Fig. 2a and b) and all measured ratios in this study (Table S1 and inset Fig. 1b, Fig. 2a and b, Fig. 4 a and b, Fig. 5b and appendix) were normalized to SRM 987 $^{87}Sr/^{86}Sr = 0.710248$, to La Jolla $^{143}Nd/^{144}Nd = 0.511858$ or Rennes $^{143}Nd/^{144}Nd = 0.511973$, and to JMC475 $^{176}Hf/^{177}Hf = 0.282160$. All Pb isotopic ratios have been normalized to the SRM 981 triple spike values of $^{206}Pb/^{204}Pb=16.9405$, $^{207}Pb/^{204}Pb=15.4963$, and $^{208}Pb/^{204}Pb=36.7219$[8]. For Sr and Nd isotopic analyses by TIMS, the normalization to the standard values was based on the mean of the standards measured during the course of a given study; SRM 987 $^{87}Sr/^{86}Sr$ and La Jolla and Rennes $^{143}Nd/^{144}Nd$ for each batch of analyses are given in Table S1.

Even though the NIST SRM 981 results were within error of the triple-spike values after online correction for instrumental mass bias by Tl addition, the results were further corrected by the sample-standard bracketing method or the ln-ln correction method as described by 1,9. The stability of the MC-ICP-MS was also controlled by monitoring the daily averages of the SRM 981 analyses (see Table 6 in 1). On average, the reproducibility of the SRM 981 was better than 110 ppm for $^{206}Pb/^{204}Pb$ and $^{207}Pb/^{204}Pb$ and better than 125 ppm for $^{208}Pb/^{204}Pb$. The in-run ±2σm errors (standard errors) were less than the ±2σ external reproducibility of the standards in all cases.

For Hf isotopic analyses, the normalization of the measured Hf ratios was based on the mean of the day of the JMC 475 analysis (n=10 to 20). Over the course of the Mauna Loa, the overall mean of $^{177}Hf/^{176}Hf = 0.282166 \pm 18$ (n=936) on the Nu 021 (Nu Instruments, Ltd.).

© 2011 **Macmillan Publishers Limited. All rights reserved.**

References

1. Weis, D. *et al.* High-precision isotopic characterization of USGS reference materials by TIMS and MC-ICP-MS. *Geochem. Geophys. Geosyst.* 7, Q08006 (2006).
2. Weis, D. *et al.* Hf isotope compositions of U.S. Geological Survey reference materials, *Geochem. Geophys. Geosyst.* **8**, Q06006 (2007).
3. Weis, D., Kieffer, B., Maerschalk, C., Pretorius, W. & Barling, J. High-precision Pb-Sr-Nd-Hf isotopic characterization of USGS BHVO-1 and BHVO-2 reference materials. *Geochem. Geophys. Geosyst.* **6**, Q02002 (2005).
4. Nobre Silva, I.G., Weis, D., Barling, J. & Scoates J.S. Leaching systematics and matrix elimination for the determination of high-precision Pb isotope compositions of ocean island basalts, *Geochem. Geophys. Geosyst.* **10**, Q08012 (2009).
5. Abouchami, W., Galer, S.J.G. & Hofmann, A.W. High precision lead isotope systematics of lavas from the Hawaiian Scientific Drilling Project. *Chem. Geol.* **169**, 187–209 (2000).
6. Nobre Silva, I.G., Weis, D., & Scoates J.S. Effects of acid leaching on the Sr-Nd-Hf isotopic compositions of ocean island basalts. *Geochem. Geophys. Geosyst.* **11**, Q09011 (2010).
7. Barling, J. & Weis, D. Influence of non-spectral matrix effects on the accuracy of Pb isotope ratio measurement by MC-ICP-MS: implications for the external normalization method of instrumental mass bias correction. *J. Anal. At. Spectrom.* **23**, 1017–1025 (2008).
8. Galer, S.J.G. & Abouchami, W. Practical application of lead triple spiking for correction of instrumental mass discrimination. *Mineral. Mag.* **62A**, 491–492 (1998).
9. White, W.M., Albarède, F. & Télouk, P. High-precision analysis of Pb isotope ratios by multi-collector ICP-MS. *Chem. Geol.* **167**, 257–270 (2000).

© 2011 **Macmillan Publishers Limited. All rights reserved.**

Supplementary Information: Sample locations.

Mauna Loa, on the island of Hawai'i, is the world's largest active volcano, rising to over 8000 m above the Pacific ocean floor. Today, it is in the tholeiitic shield-building stage and thought to have been active for the past 600-1000 kyr[1,2]. Most of Mauna Loa's eruptive activity occurs in a large summit caldera and along two narrow rift zones that extend northeast and southwest from the caldera. The northeast rift zone extends for about 40 km, where it is buried by younger Kīlauea lavas. The southwest rift zone extends for about 100 km, with 33 km below sea level descending to a depth of about 4500 m. Eruptions have also occurred from radial vents on its west and northwest flanks[3]. Giant landslides have dissected Mauna Loa's submarine flanks[4]. The ages of these landslides are poorly constrained, possibly 100 to 200 ka[2-6]. Mauna Loa's submarine southwest rift zone was cut by one of these landslides, leaving an extensive amphitheater with a 20 km long, 1.6 km high scarp exposing a thick section of pillow lavas cut by numerous thin (< 1 m) dikes[5,7,8]. This "mile high" section, the greatest surface exposure on any Hawaiian volcano, is locally capped by coral and boulders[8], constraining the minimum age of the section to between 15 and 150 ka[9,10]. The new isotope analyzes reported here are from the submarine and subaerial portions of the volcano. The submarine samples include three successive sequences of stratigraphically/controlled lavas forming the "mile high" section (89 samples) were collected during JASON2, dives J2-16, 19 and 20 and PISCES V submersible dives 184 and 185 (Fig. 3b). Recent $^{40}Ar/^{39}Ar$ dating shows that this section records about 120 to 470 ka of Mauna Loa's magmatic history[11]. Additional submarine samples were dredged during a R/V Moana Wave cruise in 1999[12] from the southwest rift zone, radial vents, the southwest slope and from landslide debris areas (Fig. 3b). From subaerial Mauna Loa, three suites of samples were analyzed: historical Mauna Loa lavas[13,14] erupted between 1843 and 1984, ^{14}C-dated prehistoric lavas ranging in age from 3 to ~37 ka[15] and five

© 2011 Macmillan Publishers Limited. All rights reserved.

samples from the pilot HSDP hole (depths within the HSDP-I hole given in m), ranging in age between 10 and 100 ka[16].

References

1. Moore, J.G. & Clague, D.A. Volcano growth and evolution of the island of Hawaii. *Geol. Soc. Am. Bull.* **104**, 1471-1484 (1992).
2. Lipman, P.W. Declining growth of Mauna Loa during the last 100,000 yr: rates of lava accumulation vs. gravitational subsidence, in *Mauna Loa Revealed: Structure, Composition, History, and Hazards* (eds: Rhodes, J.M. & Lockwood, J.P.), *Geophys. Monogr. Ser.* **92.** American Geophysical Union, Washington, DC, 45–80 (1995).
3. Lockwood, L.P. & Lipman, P.W. Holocene eruptive history of Mauna Loa volcano, in Volcanism in Hawaii (eds: Decker, R.W., Wright, T.L., Stauffer, P.H.), U.S. Geol. Surv. Prof. Paper 1350, 509-535 (1987).
4. Moore, J.G. *et al.* Prodigious submarine landslides on the Hawaiian Ridge. *J. Geophys. Res.* **94**, 17465-17484 (1989).
5. Moore, J.G. & Chadwick W.W. Offshore geology of Mauna Loa and adjacent areas, Hawaii, in *Mauna Loa Revealed: Structure, Composition, History, and Hazards* (eds: Rhodes, J.M. & Lockwood, J.P.), *Geophys. Monogr. Ser.* **92.** American Geophysical Union, Washington, DC, 21-44 (1995).
6. McMurtry, G. *et al.* Stratigraphic constraints on the timing and emplacement of the Alika 2 giant Hawaiian submarine landslide. *J. Volc. Geotherm. Res.* **94**, 35-58 (1999).
7. Fornari, D., Malahoff, A. & Heezen, B. Submarine slope micromorphology and volcanic substructure of the Island of Hawaii inferred from visual observations made from U.S. Navy deep-submergence vehicle (DSV) “Sea Cliff”. *Marine Geol.* **32**, 1-19 (1979).
8. Garcia, M.O., Hulsebosch, T.P. & Rhodes, J.M. Olivine-rich submarine basalts from the southwest rift zone of Mauna Loa volcano: implications for magmatic processes and geochemical evolution, in *Mauna Loa Revealed: Structure,*

© 2011 **Macmillan Publishers Limited. All rights reserved.**

Composition, History, and Hazards (eds: Rhodes, J.M. & Lockwood, J.P.), *Geophys. Monogr. Ser.* **92.** American Geophysical Union, Washington, DC, 219–239 (1995).

9. Moore, J.G., Normark, W.R. & Szabo, B.J. Reef growth and volcanism on the submarine southwest rift zone of Mauna Loa, Hawaii. *Bull. Volc.* **52**, 375-380 (1990).
10. Webster J.M. *et al.* Drowning of the –150 m reef off Hawaii: A casualty of global meltwater pulse 1A? *Geology* **32**, 249-252 (2004).
11. Jicha, B., Rhodes, J.M., Singer, B.S., Vollinger, M.J. & Garcia, M.O. $^{40}Ar/^{39}Ar$ geochronology of submarine Mauna Loa volcano, Hawaii. American Geophysical Union, Fall Meeting, abstract #V43F-2328 (2009).
12. Davis, M.G., Garcia, M.O., Wallace, P., Volatiles in glasses from Mauna Loa, Hawaii: Implications for magma degassing and contamination, and growth of Hawaiian volcanoes. *Contrib. Mineral. Petrol.* **144**, 570-591 (2003).
13. Kurz, M.D. *et al.* Isotopic evolution of Mauna Loa volcano: a view from the submarine southwest rift zone, in *Mauna Loa Revealed: Structure, Composition, History, and Hazards* (eds: Rhodes, J.M. & Lockwood, J.P.), *Geophys. Monogr. Ser.* **92.** American Geophysical Union, Washington, DC, 289–306 (1995).
14. Rhodes, J.M. & Hart, S.R. Episodic trace element and isotopic variations in historical Mauna Loa lavas: implications for magma and plume dynamics, in *Mauna Loa Revealed: Structure, Composition, History, and Hazards* (eds: Rhodes, J.M. & Lockwood, J.P.), *Geophys. Monogr. Ser.* **92.** American Geophysical Union, Washington, DC, 263-288 (1995).
15. Lockwood, J. P. Mauna Loa eruptive history – the preliminary radiocarbon record, in *Mauna Loa Revealed: Structure, Composition, History, and Hazards* (eds: Rhodes, J.M. & Lockwood, J.P.), *Geophys. Monogr. Ser.* **92.** American Geophysical Union, Washington, DC, 81-94 (1995).

© 2011 **Macmillan Publishers Limited. All rights reserved.**

16. Sharp, W.D., Turrin, B.D., Renne, P.R. & Lanphere, M.A. The $^{40}Ar/^{39}Ar$ and K/Ar dating of lavas from the Hilo 1-km core hole, Hawaii Scientific Drilling Project, *J. Geophys. Res.* **101**, 11,607-11,616 (1996).

© 2011 **Macmillan Publishers Limited. All rights reserved.**